



Team INDRA - Project VAJRA
Team B Final Design Report for Subscale 2025

Shaurya Mittal¹, Shaunik Purkayastha², Tushit Chatterjee³, Krishanu Dey⁴, Dhruv Phalod⁵,
Vanshdeep Trivedi⁶, Mutra Sai Tharun⁷, Rudra Rajpurohit⁸, Swaraa Sule⁹,
Adithya Adiga¹⁰

1 Aerodynamics Member

2 Propulsion Member

3 Structures Member

4 Avionics Member

5 Avionics Member

6 Avionics Member

7 Payload Member

8 Payload Member

9 Management Member

10 Management Member

Team Indra's rocket, Vajra, is powered by an N3452 N-class SRAD rocket motor. Its internal frame is made from Aluminum 6061, and the aerodynamic structure combines Carbon Fibre and Glass Fibre for optimal performance. The nosecone houses a CanSat payload with a GIMBAL-controlled platform, attached via springs to withstand rocket vibrations. An onboard microcontroller ensures the platform is positioned to keep a PYRAMID object aligned with the camera's center for tracking the entire flight. The avionics use Surface Mount Technology (SMT) components, with two microcontrollers handling tasks like data logging, apogee detection, recovery control, and airbrake activation. The flight computer supports real-time telemetry up to 16 kilometers, transmitting flight dynamics and GPS data.

NOMENCLATURE

COTS- Commercial Off The Shelf

SRAD- Student Researched And Developed

DoF- Degree of Freedom

IMU- Inertial Measurement Unit

GPS- Global Positioning System

FSM- Finite State Machine

LiPo- Lithium-Polymer

PCB- Printed Circuit Board

SMT- Surface Mount Technology

PSRAM- Pseudo-Static Random Access Memory

I2C- Inter-Integrated Circuit

SPI- Serial Peripheral Interface

UART- Universal Asynchronous Receiver Transmitter

ODR- Output Data Rate

MEMS- Micro-Electro-Mechanical Systems

RF- Radio Frequency

LoRa- Long Range

GNSS- Global Navigation Satellite System

CNC - Computerized Numerically Controlled

M - Metric size

Al - Aluminium

mm - millimetres

in - inches

Ft - feet

nos. - numbers

WPC - Wood Plastic Composite

ID - inner diameter

CFRP - Carbon Fiber Reinforced Polymer
OD- Outer Diameter
GFRP- Glass Fiber Reinforced Polymer
MPU- Motion Processing Unit
SD- Secure Digital
PDB- Power Distribution Board
BEC- Battery Eliminator Circuit
LOS- Line of sight
PID- Proportional Integral Derivative
PWM-Pulse Width modulation
GND- Ground
SDA- Serial Data
SCL- Serial Clock
RX- Receive
TX- Transmit
FR4- Flame Retardant 4
SMD- Surface Mounted Device
LED- Light Emitting Diode
I2C- Inter-Integrated circuit
CFD- Computational Fluid Dynamics
CP- Center of Pressure
CG- Center of Gravity
Cd- Coefficient of Drag
T₉₉- Thickness of boundary layer
L_c- Characteristic length of body
Re - Reynolds number
ρ - Density
ABS - Acrylonitrile Butadiene Styrene
GLONASS- Globalnaya Navigatsionnaya Sputnikovaya Sistema

I. INTRODUCTION

Team Indra is a student-run rocketry team in Manipal, India. We are named after one of the mightiest and strongest gods in Hindu mythology. With access to state-of-the-art resources and immense hardwork, our diverse and talented team is exceptionally equipped to tackle the complex engineering challenges of rocketry. We have a mission, to create a fully functional sounding rocket that reaches a height of 10,000 feet. We are dedicated to using our collective creativity and determination to fulfil our purpose and further develop groundbreaking solutions that advance the field of aerospace engineering.

II. SYSTEM ARCHITECTURE OVERVIEW

Vajra is a solid propellant rocket standing 2.64 m tall with an outer diameter of 14.4 cm and a pad mass of 37.7 kg. The rocket body is made up of 2 modular body tubes. The body tubes have been manufactured from CFRP to keep them lightweight while providing significant structural strength to withstand the various loads acting on the rocket during its flight and one of the body has been manufactured using GFRP to support avionics telemetry. The rocket is powered by a N-3452 SRAD N-class motor.

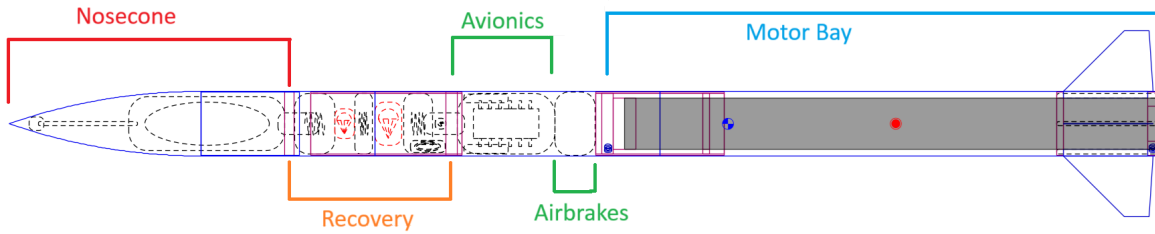


Fig 1: OpenRocket layout of Vajra

A. Aerodynamics

1. Nosecone

A nosecone's primary function is to reduce a rocket's drag by providing a streamlined profile. The material chosen for the nosecone was carbon fibre. Several nosecone profiles were considered for use in this rocket. These nosecones were -

Nosecone Profile
Tangent Ogive
Von Karman
Power 1/2
Power 3/4

Table 1 : Nosecone profiles considered for simulations

CFD simulations were used to determine the drag characteristics of these 4 profiles. These simulations were carried out for a fineness ratio of 3:1 and velocity of 280 m/s.

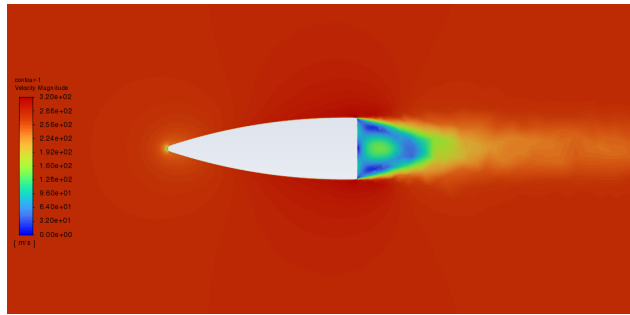


Fig 2: Velocity plot for Tangent Ogive nosecone at 280 m/s

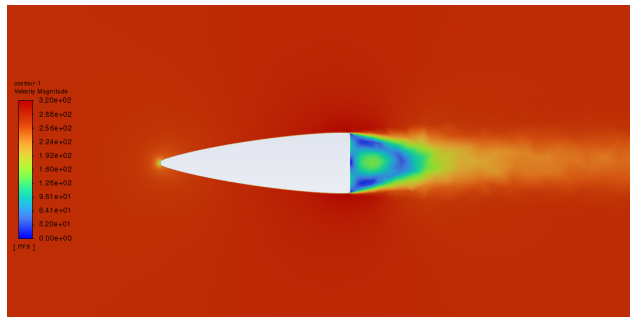


Fig 3: Velocity plot for Von Karman nosecone at 280 m/s

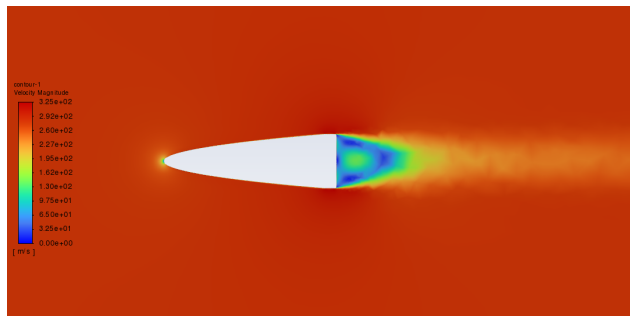


Fig 4: Velocity plot for Power Series $\frac{1}{2}$ nosecone at 280 m/s

The CFD yielded the following results -

Nosecone Profile	Coefficient of Drag
Tangent Ogive	0.157
Von Karman	0.159
Power 1/2	0.1635
Power 3/4	0.1686

Table 2 : CFD results for the considered nosecone geometries.

From this data, it was concluded that Tangent ogive nosecone was the best profile with the least drag and hence was used in the rocket. The outer diameter of the nosecone was 14.4 cm and the length was 43.2 cm.

Due to manufacturing limitations of carbon fibre, the tip of the nosecone was manufactured with a bluffness ratio of 0.1 using aluminium.



Fig 5 : Aluminium nosetip used with the tangent ogive nosecone with bluffness ratio 0.1

2. Fins

This rocket uses 4 trapezoidal fins with a rounded cross section near the base of the motor bay. The primary function of these fins is to pull the CP of the rocket near the base and away from the CG. This is done to increase the stability of the rocket. When flown with optimal stability margin, the rocket reliably remains upright throughout the flight and achieves maximum apogee.

OpenRocket software was used to determine the optimal dimensions for the fins which would allow the rocket to achieve an apogee of 10,000 ft while maintaining a safe stability margin.

Shape	Trapezoidal with rounded cross-section
Material	Aluminium 6061
Root Chord	20 cm
Tip Chord	5.5 cm
Semi Span	13.4 cm
Thickness	0.27 cm (2.7 mm)
Sweep Angle	45°

Table 3 : Fin Dimensions used in the rocket

To avoid damage to the fins due to Fin Flutter, FinSim software was used to calculate the fin flutter velocity of the rocket. At fin flutter velocity, the fins oscillate at the highest amplitude and break as a result of the deformation. To avoid this, the rocket needs to fly at a velocity lower than the fin flutter velocity. For a fin thickness of 2.7 mm (0.106 inch), the fin flutter velocity was found to be 438 m/s at maximum drag conditions at 1000 ft. For the maximum rocket velocity of 283 m/s, a safety factor of 1.54 was achieved.

3. Air Brakes

This rocket is designed to intentionally overshoot the prescribed apogee of 10,000 ft so that an aerodynamic braking system can be implemented to precisely lower the apogee of the rocket by actively predicting the apogee and deploying the airbrakes.

The airbrake employs a slider-crank mechanism to slide two brake plates out of the rocket body which experience drag due to the moving air around the body which slows the rocket down.

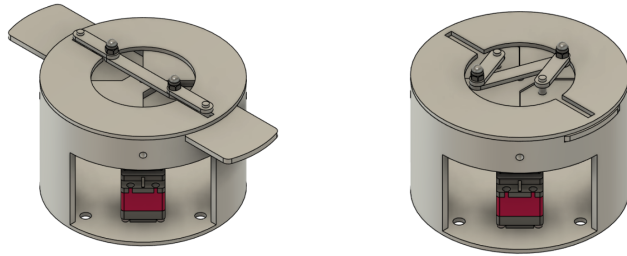


Fig 6 & 7: The airbrakes in deployed and retracted configuration

To determine the appropriate surface area for the airbrake plate and Cd, initially a flat plate approximation of 1.28 Cd was used.¹ The system was designed to enable aerodynamic breaking at the altitude of 6500 ft at a Then Matlab R2024a was used to analyse the capacity of different configurations of airbrakes to lower the apogee of the rocket. The initial conditions for the code was the following -

Initial Altitude	6500 ft
Initial velocity	157 m/s
Cd of the rocket	.44
Frontal area of the rocket	0.0168 m ²

Three configurations were considered - 2 plate, 3 plate and 4 plate.

Through the results of the Matlab code, a range of surface area and Cd was obtained for which the airbrake was able to reduce its apogee from the initial predicted maximum apogee to the prescribed apogee of 10,000 ft (3048 m).

¹ [NASA Glenn Research Center - Shape Effects on Drag](#)

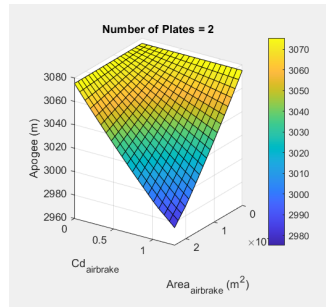


Fig 8 : Airbrake simulations for 2 plate configuration.

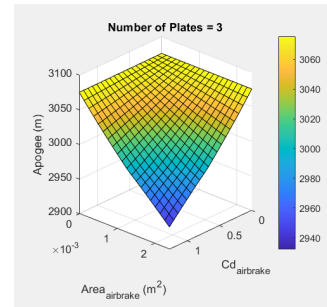


Fig 9 : Airbrake simulations for 3 plate configuration.

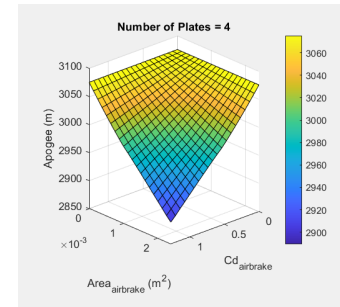


Fig 10 : Airbrake simulations for 2 plate configuration.

A plate of 4 cm x 6 cm was chosen for the airbrakes from the obtained data. For the surface area of 24 cm² it was found that with 2 plates, the system would be able to reduce the apogee of the rocket to the optimal level with any Cd above 0.34.

CFD simulation was carried out to validate these findings and determine the Cd of the plate protruding outside the body tube.

The CFD yielded a Cd of 0.988 which was in the range of optimal Cd for the airbrake for which it has the capacity to lower the apogee from the initial predicted apogee to 10,000 ft.

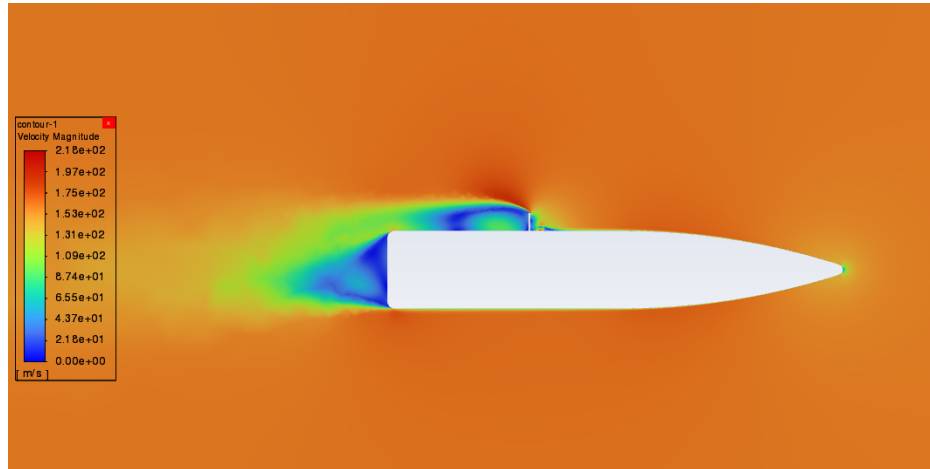


Fig 11 : Velocity contour of a single airbrake plate deployed from the body tube at 161 m/s.

4. Aerocover

This rocket is equipped with two aerodynamic covers which house the Pitot tube for airspeed measurement and a camera for capturing on-board footage.

The material chosen for the aerocover was ABS plastic which provides the ability to use 3D printing for the manufacturing of the cover. The aerocover profile contains 45 degree inclinations to improve the drag characteristics of the body.

The pitot tube needs to be positioned outside the boundary layer of the rocket since the boundary layer around the rocket experiences flow slower than the flow outside the boundary layer and can yield incorrect measurements.

$$T_{99} = 0.38 \cdot \frac{l_c}{\sqrt[5]{Re}} \quad Re = \frac{\rho U l_c}{\mu}$$

$$\frac{0.38 \times 0.144}{\left(\frac{1.16 \times 280 \times 0.144}{0.00001784}\right)^{0.2}} = 2.84 \times 10^{-3} = 2.84 \text{ mm}$$

For the conditions at maximum drag, density at 1500 ft was taken as 1.16 Kg/m³. Maximum velocity of 280 m/s was considered and these calculations² yielded a boundary layer thickness of 2.84 mm and the pitot tube was accordingly.

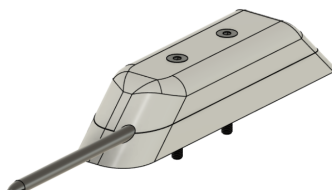


Fig 12: Fully assembled aerocover with pitot tube and camera

² Introduction to Flight by John D Anderson p 210

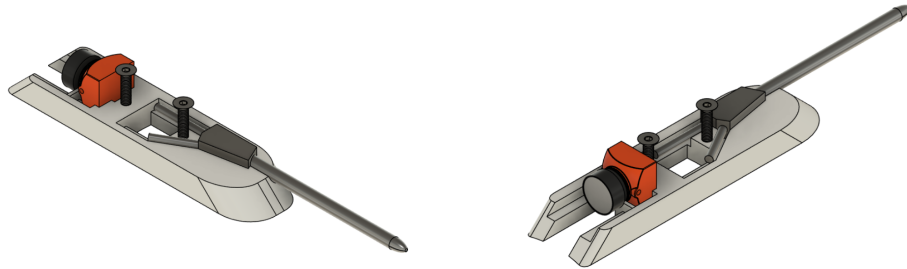


Fig 13 & 14: Aerocover without the top cover with the view of the camera and the pitot tube seated

CFD simulation was carried out to determine the Cd of the aerocover. The results yielded a Cd of 0.2779 which was used in the OpenRocket simulations.

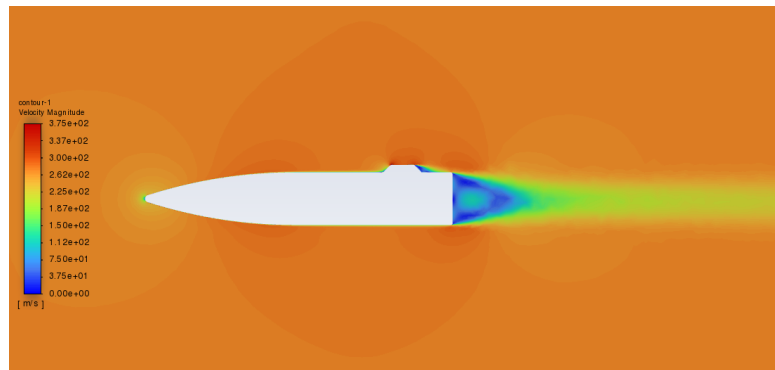


Fig 15 : Velocity contour of the aerocover at 280 m/s

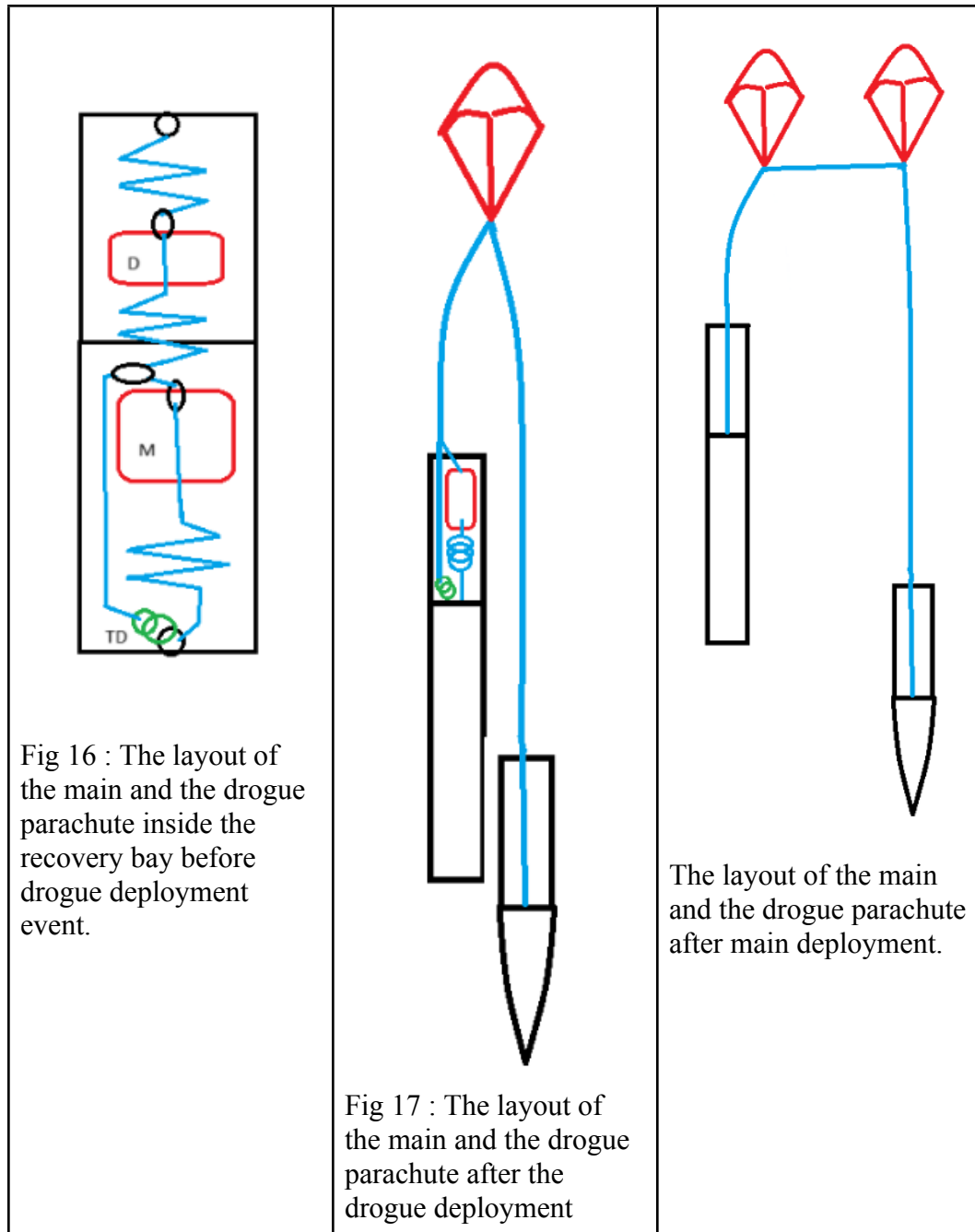
5. Recovery

To recover the rocket safely from an altitude of 10,000 ft, this rocket utilises a dual event deployment system using two L2 Tender Descenders connected in series. The recovery system comprises of two parachutes, one Elliptical 24" Parachute from Fruity Chutes with a Cd of 1.55 as a drogue and a 66" Iris Ultra parachute with a Cd of 2.2 from Fruity Chutes as the main parachute.

The drogue parachute is attached to the recovery bulkhead through 300 cm of kevlar 6.4 mm shock cord and two L2 tender descenders in series for redundancy. The drogue is attached to the nosecone bulkhead through a 600 cm kevlar 6.4 mm shock cord rated at 2200 lb. These attachments are made through M10 stainless steel shouldered screw eyebolts. The maximum achieved descent velocity after drogue deployment was found to be 36.6 m/s.

The main parachute is attached to the recovery bulkhead through 900 cm of Kevlar 6.4 mm shock cord rated at 2200 lb. The main parachute is also connected to the drogue line so that it is constrained inside the body tube and doesn't get pulled out of the body tube before the main event.

At main deployment event, the tender descenders are triggered which detaches the drogue from the recovery bulkhead and allows the drogue to pull the main parachute out and deploy the main parachute.



	event.	
--	--------	--

B. Structures

Thrust Plate:

Thrust Plate is the component taking up the Load provided by the Thrust of the Solid Rocket Motor (Reference) during the Powered Flight i.e.- when the Solid Rocket motor is providing thrust. The Thrust Plate is made up of Aluminium 6061 T6 and is intended to be CNC milled to the required geometry. Al 6061 T6 is chosen because it has a high strength while being light in weight which becomes a crucial deciding factor in the rocket body.

The Thrust Plate has a 12mm (0.472 in.) hole at the centre of it in which an M12 bolt is supposed to go and thread down to the Forward Closure (Reference) bolt hole, hence, providing it forward retention as well as centring the rocket motor.

The Thrust Plate itself is of 136mm (5.354 in.) in diameter and 30mm (1.181 in.) in thickness considering a high factor of safety as it is the first point of contact of the thrust force provided by the rocket motor. The thickness is kept high to ensure that the high thrust of the motor does not elongate the bolt holes or result in a tear-out of the radial bolts. To reduce the motor vibration and effect of vibrations on the Thrust Plate of the rocket, a WPC Damper (Reference) is used between the rocket motor and thrust plate inside the forward closure cavity.

Thrust Plate is attached to the body using 4 nos. M6 course threaded grade 8.8 bolts to transmit the thrust force provided by the solid rocket motor to the entire body of the rocket. A Standard 1515 Rail button is attached to the Thrust plate for which an additional M8 size bolt hole is provided.

The Thrust plate design is simulated on ANSYS Static Structural Module to ensure the expected results. Results of which are provided in Appendix (Alphabet).

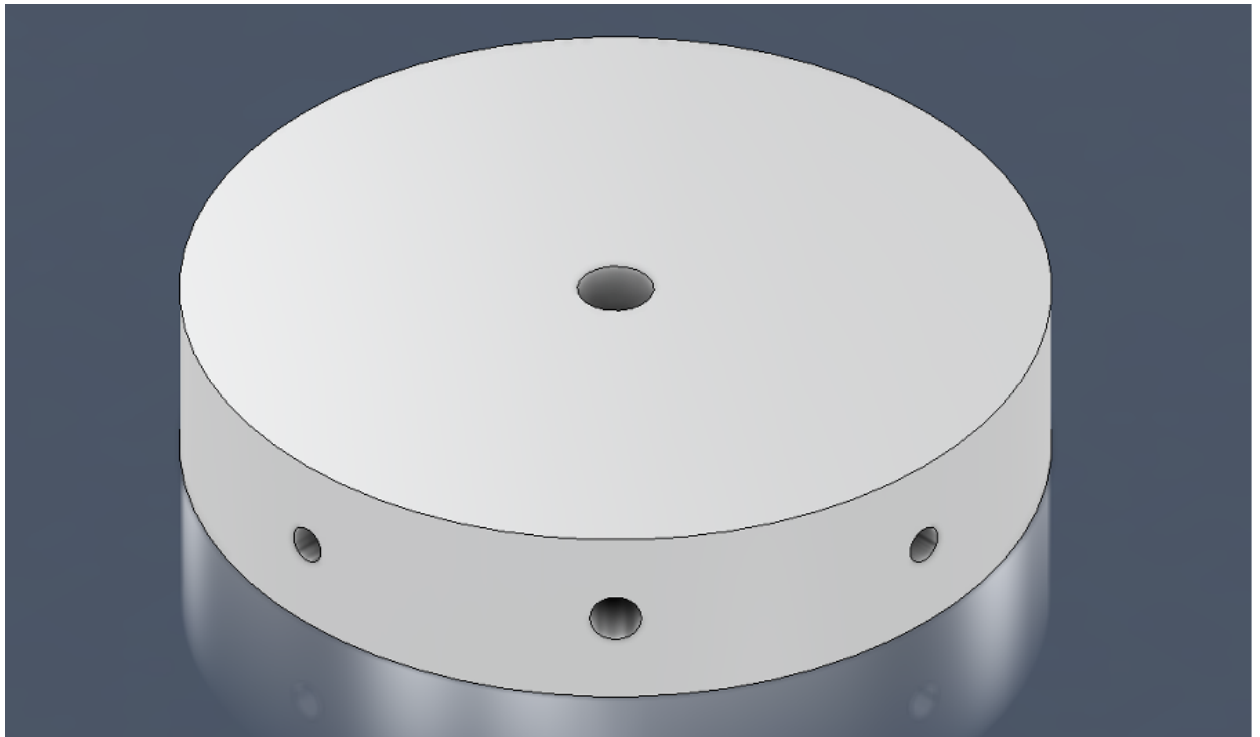


Figure 16: Thrust Plate

Forward Centring Ring:

There are 2 centring rings installed in the rockets to ensure ease of assembly and proper centring of the solid rocket motor. The centring ring has some clearance from the Motor casing so that during assembly of the motor the Bolt heads on the motor casing can also pass through the ID of the ring. The ID of the centring ring is hence, 121mm (4.763 in.). The OD of the ring is kept as 136mm (5.354 in.) so that it fits inside the Motor Bay Coupler (Reference).

The forward centring ring has M3 Bolts on it for radially bolting it to the coupler and Motor Bay body tube (Reference). The centring ring has small radial bolt holes because it is not a load bearing member in the rocket body rather, it is just there to keep the rocket motor centred as well as useful for attaching the coupler to motor bay body tube.

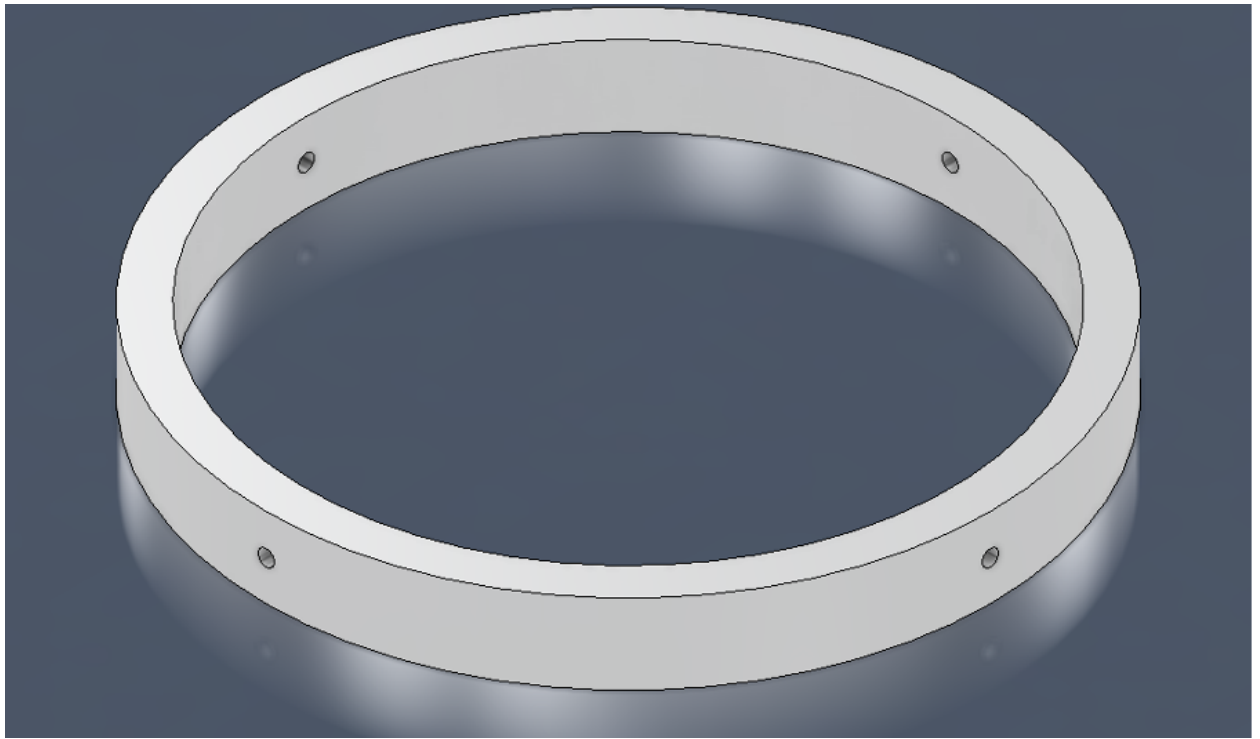


Figure 17: Forward Centring Ring

Aft Centring Ring:

Aft centring ring is part of the Fin Can Assembly (Reference) that ensures that the fins are properly aligned with respect to the body of the rocket. The aft centring ring has slots cut on it using Milling operation to attach the Stringer (Reference) and Welded fin assembly to it.

The Aft centring ring has an OD of 140mm (5.511 in.) and an ID of 121mm (4.763 in.) and is attached directly to the motor Bay body tube using M3 radial bolts.

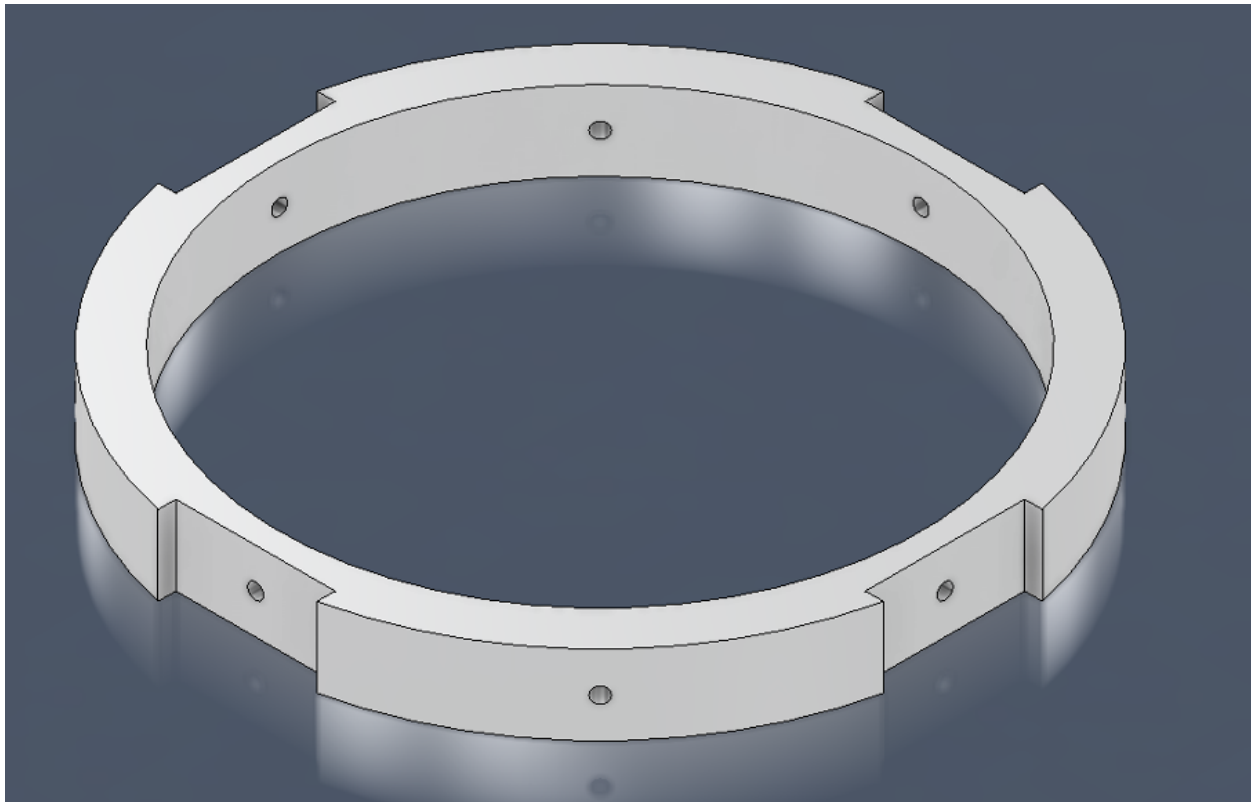


Figure 18: Aft Centring Ring

Retainer:

Although there is forward retention provided for the motor using M12 Axial bolt at forward closure, for keeping the rocket motor completely intact in the Motor Bay, an additional layer of Motor retention is added using Retainer that holds the rocket motor inside a contraption on which the motor sits. The inner diameter of the retainer is kept as 121mm (4.763 in.) in where the motor casing will be sitting. There is a clearance between the casing and retainer wall to accommodate the Bolt heads within the inner diameter of the retainer.

The retainer has an 88mm (3.464 in.) hole at the bottom of it from which the nozzle of the rocket is coming out as the casing sits on the retainer.

The Retainer has slots cut in it to make space for the Stringer Fin Assembly as the retainer is also part of the Fin Can.

The retainer is attached to the Body tube using M5 Bolts bolted Radially and is directly attached to the CFRP Body Tube.

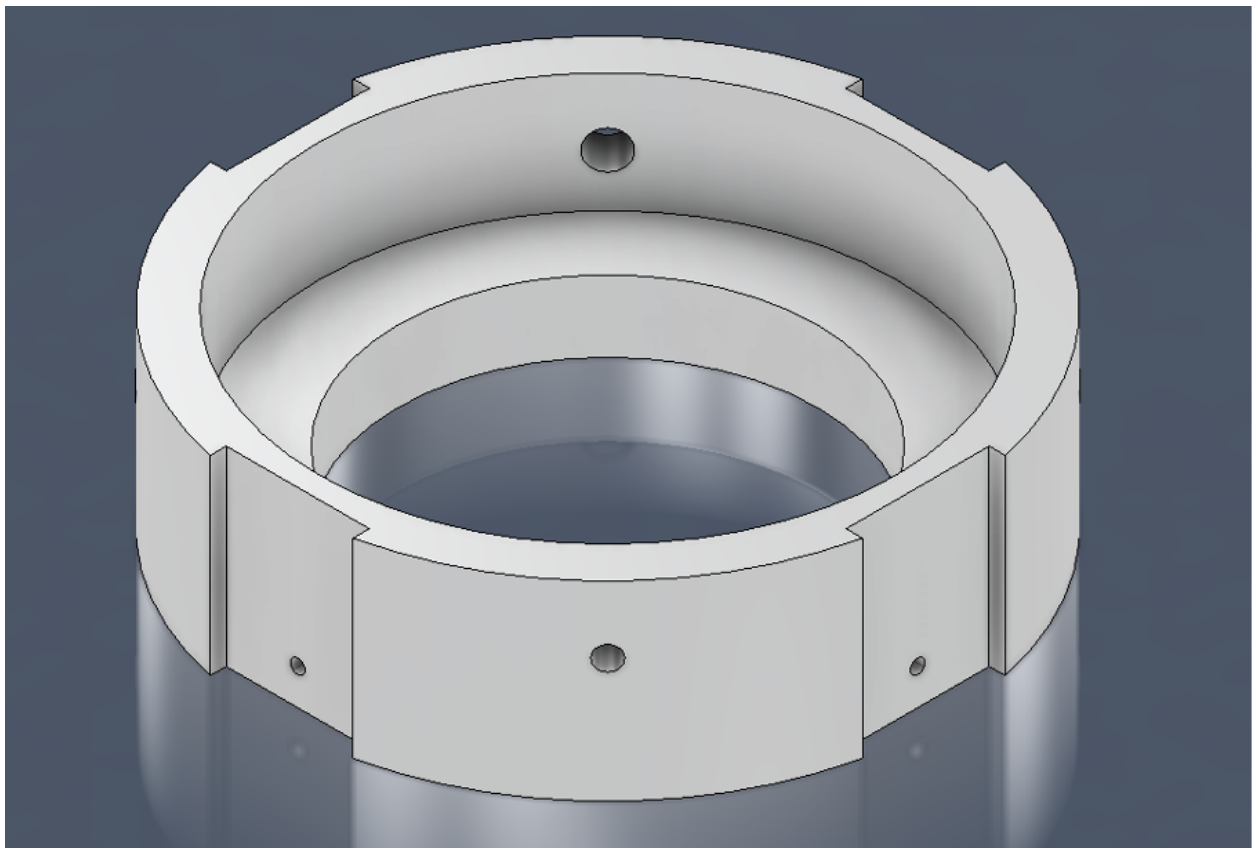


Figure 19: Retainer

Fin Can Assembly:

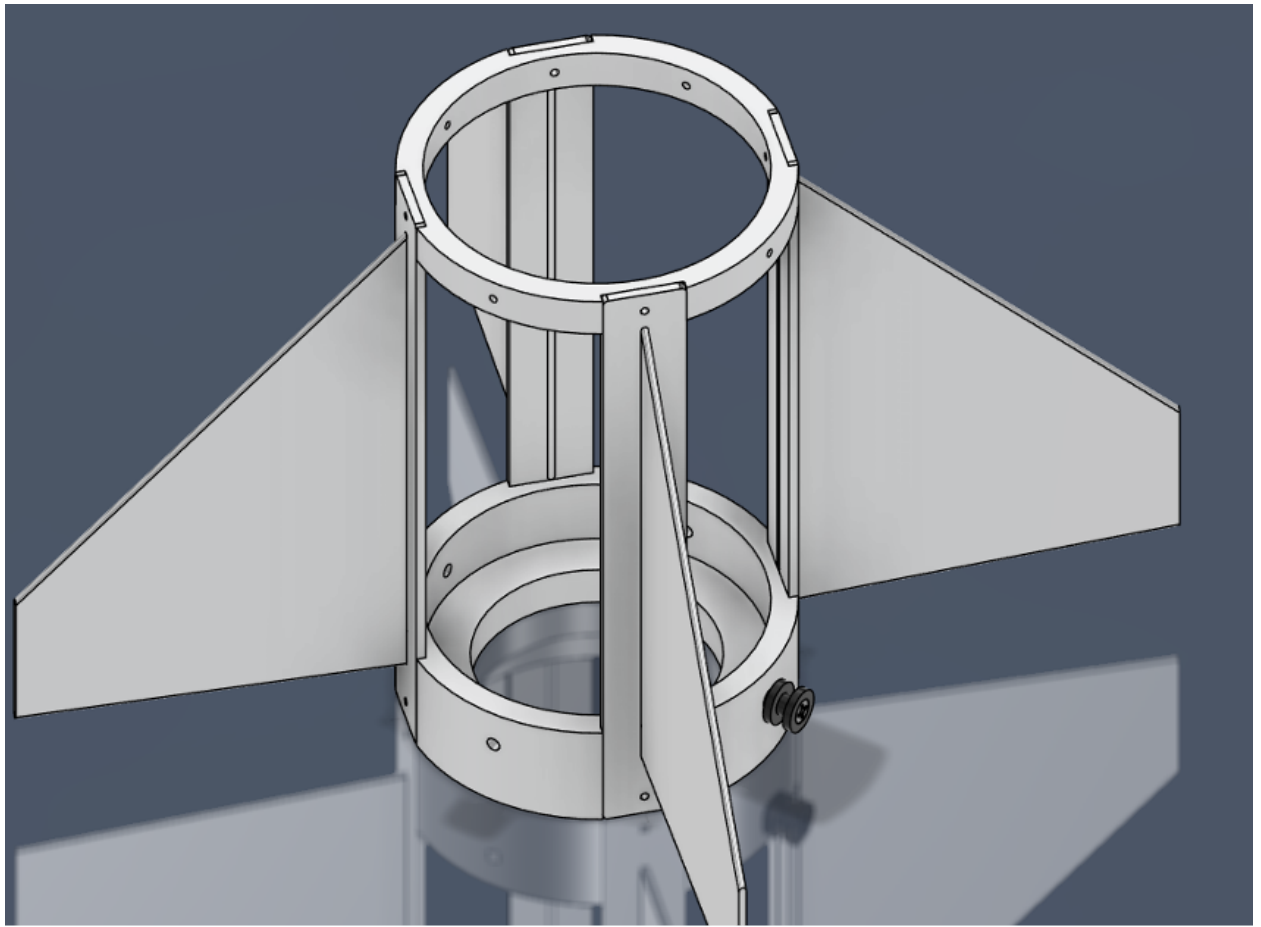


Figure 20: Fin Can Assembly

The Fin Can Assembly consists of Retainer, Centring ring and the assembly of 4 stringers. Stringers are made of Aluminium 6061 T6. Slots are cut on the stringers using CNC Slot milling to align fin tabs. Stringers are welded with aluminium fins to align them axially to the rocket body.

Both retainer and centring ring go around the motor and houses Rail buttons as well.

Motor Bay Body Tube:

Motor Bay is made from Carbon Fiber Reinforced Polymer Composite material manufactured using Hand Lay-up method. The Carbon Fiber is of 210 GSM 2*2 Plain woven fibre. The specific one was chosen based on availability and Buckling Calculator (Reference) was used to do Bucking calculations on cylindrical body tube to get the thickness of the body tube.

The tube has slots cut into it so that the Fin Can assembly can slide in the motor bay from outside the body tube i.e. the Fin Can assembly is assembled outside the body and slid into the body tube. Radial holes are made on the body tube to give space to the radial bolts to go in and mount the Fin Can from the Radial Bolts on Retainer and Centring Ring.

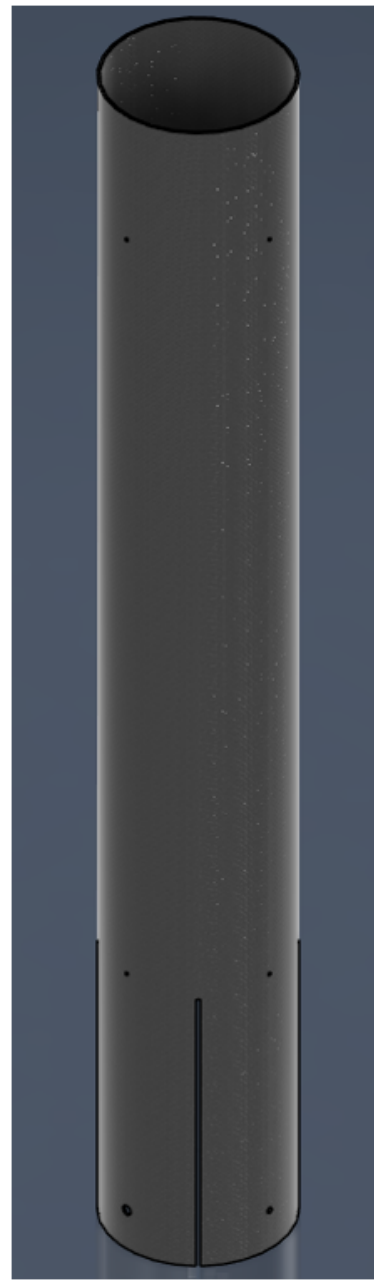


Figure 21: Motor Bay Body Tube

Motor Bay Coupler:

Motor Bay Coupler is made up of CFRP using Hand Lay-up method and radial holes are made on it to specified dimensions and positioning provided in the Engineering Drawings (Reference).

The coupler goes into the motor bay body tube by 1 cal. i.e. the length of the coupler that goes inside the body tube is equal to the OD of the Rocket.



Figure 22: Motor Bay Coupler

Damper:

Damper is made out of WPC material this is because WPC has a porous structure while having a Poisson's ratio of 0.2 to 0.3 which means it has a lot of space within the material to compress under loading while expanding radially outward. But the damper cannot expand

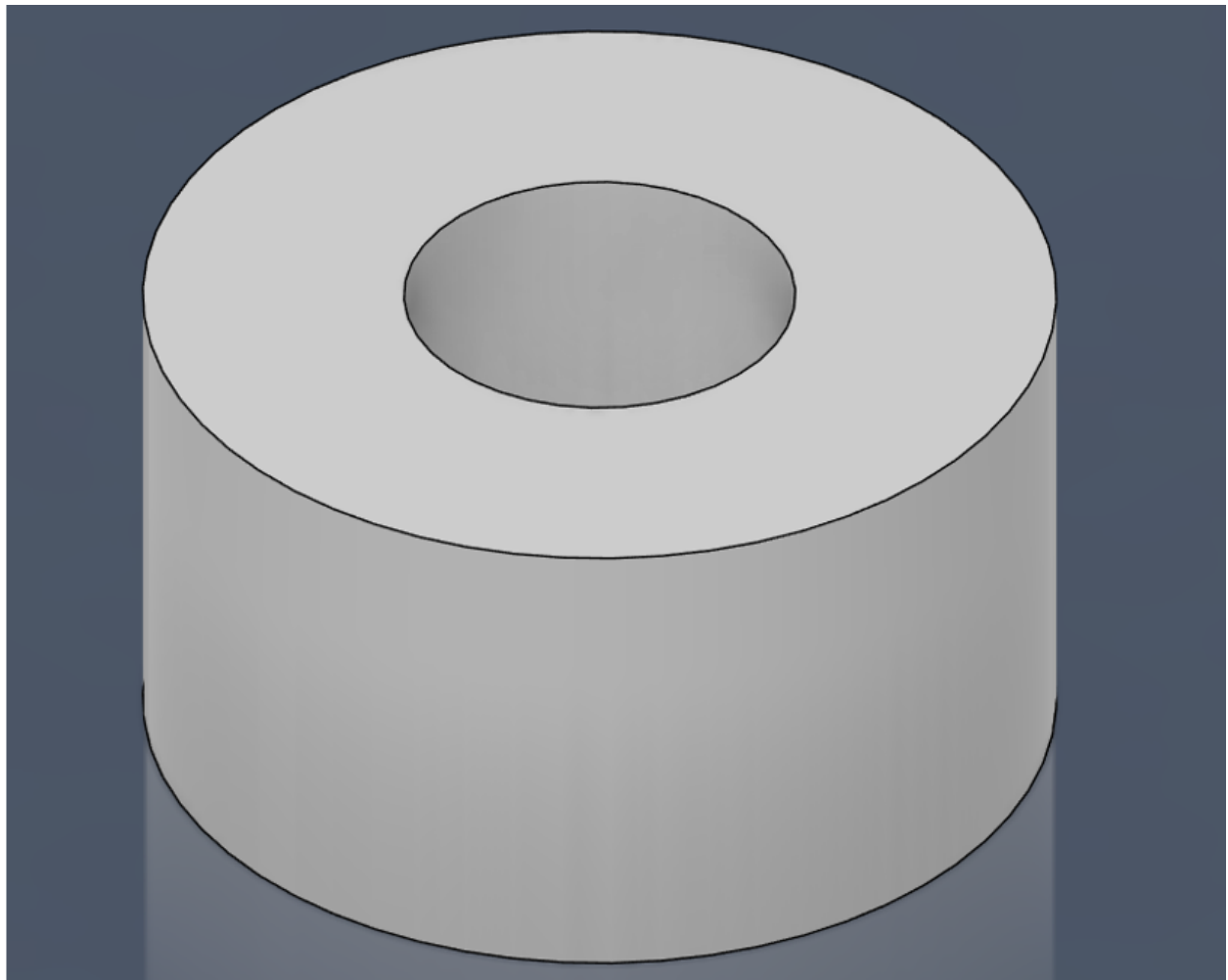


Figure 23: Damper

radially outward because of the walls of Forward closure. Thus, making it perfect for dampening purposes. Therefore, a Damper is constructed out of it which comes in between the motor and Thrust plate to dampen the residual vibrations of the rocket motor.

Manufacturing of the damper is done on lathe machine where it is turned down to the required OD and then Boring is done to bring ID to the specified ID.

Recovery Bulkhead:

The Recovery bulkhead is made from milling of Al 6061 T6. There are 2 nos. of charge wells on the Recovery Bulkhead one will be used for the main deployment charge and the other will be the redundancy charge. The design is made in such a way that the igniters from the avionics bay can come through the 3mm holes in the charge well from the avionics bay.

The diameter of the recovery bulkhead is 136mm (5.354 in.) and the thickness of the bulkhead is 25mm (0.984 in.). This thickness is taken by taking a high factor of safety because during the deployment event high pressure will be generated by the burning of the black powder and the structure should withstand it without the Radial bolt holes elongating or tearing out. Moreover, since a Tender Descender system is used, that needs to be connected to the avionics through wires, a small 3mm hole is made on the recovery bulkhead that matches with the similar hole in avionics mount that can be used to pass wires through it from avionics to tender descenders.

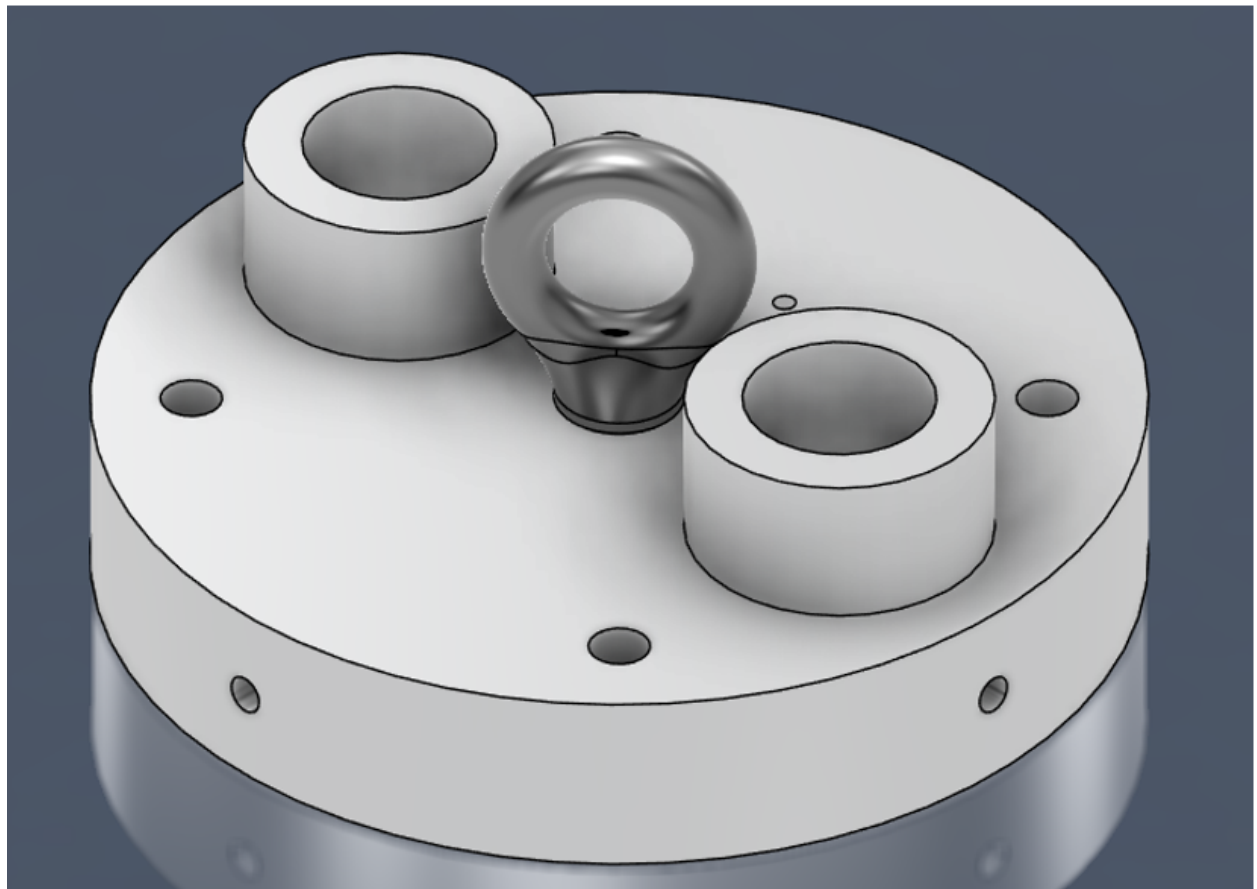


Figure 24: Recovery Bulkhead

4 holes each of a diameter of 8mm (0.314 in.) is carved out of the bulkhead axially to have threaded rods pass through them which will hold the Avionics mount below it securely using nuts. One hole of 10mm (0.393 in.) is made at the centre of the Recovery Bulkhead for an M10 eye bolt to thread down in it.

Radially, M5 bolts are used to fasten the bulkhead to the rest of the rocket body. This size is calculated from Bolt calculation formulae (Reference).

Avionics Bay Body Tube:

Avionics Bay body tube is made from fiberglass and consists of bolt holes for joining Thrust Plate, Airbrakes, rail buttons and recovery bulkhead. Moreover, it consists of 2 slots for airbrakes to come out of it when needed, it also contains cut-outs for the Aero cover to Mount on it and the pipes to pass through it.

The Fiberglass body tube is chosen for the ease of communication as it is optically transparent.



Figure 25: Avionics Bay Body Tube

C. Propulsion

I. System Architecture Overview

A. Propulsion

The propulsion system of Vajra is equipped with a SRAD "N3452" solid rocket motor using KNSB as the propellant of choice with a total impulse of 10773.34 N-sec. The maximum thrust is 3847.27 N and the average thrust is 3452 N. The thrust-time curve of the designed motor shows progressive behavior with a burn time of 3.09 seconds and a maximum expected operating pressure of 5.47 MPa. The motor casing is made from Aluminum 6061-T6 alloy; the outer diameter of the motor casing is 114 mm with 6.5 mm thickness. The headliner is made up of CFRP and is 3 mm thick. A 1.5 mm thick CRPF liner is used for thermal insulation, which reduces the heat transfer between the combustion chamber and the casing. O-rings are used in the nozzle and the forward closure to form a seal and prevent any pressure leak. KNSB is used as the propellant, having sorbitol as the fuel and potassium nitrate as the oxidizer in the ratio 65:35 by weight. Four grains were made with each grain length being 240 mm with the core diameter being 50 mm. Material for the forward closure is Aluminum 6061-T6, and the nozzle is made of stainless steel. Bolts have been used as a method of attachment. Bolt calculations were done, and the minimum number of bolts required was found to be 6×M6 bolts of grade 10.9. To ensure that the design is failsafe, it was decided that 12 bolts should be used for fastening both, the nozzle and the forward closure, hence increasing the factor of safety. M6 bolts of grade 10.9 are used. Total length of the motor is 1160 mm, and mass of the propellant is 9.06 kg.



Fig. 26: N3452 Rocket Motor

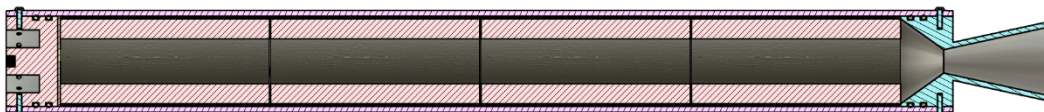


Fig. 27: N3452 Rocket Motor: Section View

The motor consists of the following components: casing, liner, propellant grain, nozzle, and forward closure.

Casing

motor casing is made of 6061-T6 aluminum, with an external diameter of 114 mm, a height of 1086.5 mm, and a thickness of 6.5 mm. The casing is designed to withstand a pressure of 8.5193 MPa. The MEOP considered while designing the rocket motor was 5.6795 MPa. The factor of safety is taken as 1.5.

The forward closure is made of 6061-T6 aluminum. This alloy was chosen due to its favorable strength-to-weight ratio, availability and affordability. A M12 threaded hole is placed in the center of this component to facilitate forward retention of the motor.



Fig. 28: Forward Closure.

The O-ring used for sealing the motor has the identification code 2-342 from Parker. It has an internal diameter of 91.4 mm and a cross-sectional diameter of 5.33 mm. The O-ring guaranteed low gas permeability and hence tight pressure sealing within the combustion chamber. In addition to the O-ring, a small amount of high-temperature RTV silicone is applied as an easy way to check for leaks after the motor operation. The O-ring was sized using hand calculations

as recommended by the Parker O-ring handbook, the results of which were verified using the Parker O-Ring Selector.

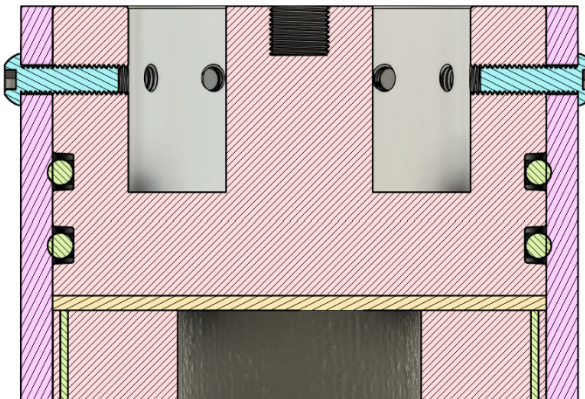


Fig. 29: O-ring slots in the forward closure

Nozzle

The nozzle is made of AISI 316 stainless steel, has a throat of 26 mm in diameter and 1 mm in length, a converging half-angle of 35° and a diverging half-angle of 12° , and an exit diameter of 78 mm.

The alloy has a yield strength of 205 MPa and a minimum rupture strength of 97 MPa at a temperature of 600°C . With these characteristics, it becomes a good option for the nozzle.

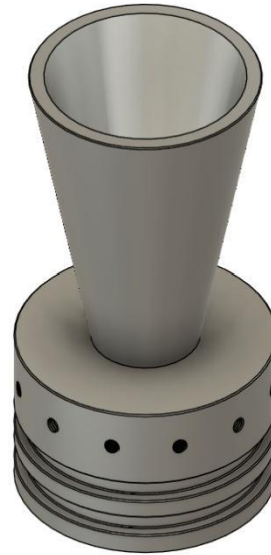


Fig. 30: Nozzle

Thermal Liner

The thermal liner is a crucial component that prevents heat transfer to the motor casing. Its insulation prevents heat generated from the propellant combustion from causing structural damage to the combustion chamber. A 1.5 mm thick CFRP liner is used around the inner diameter of the casing. A 101 mm diameter and 3 mm thick disc of CFRP is also used to protect the forward closure.

Four CFRP casting tubes of thickness of 1.5 mm and an ID of 95 mm, each 240 mm long are used for propellant casting, and inhibition. Three O-rings of cross section 1.5 mm and ID 95 mm are used between each grain as spacers to allow the end faces of the grain to burn.

Internal Ballistics

The motor features a 4-segment BATES grain geometry configuration. All segments are 240 mm in length have an OD of 95 mm. All the segments have a core diameter of 50 mm. This setup was first designed using Richard Nakka's SRM.xlsx and was simulated in an open-source software, OpenMotor.

Some of the most important parameters that were considered when designing the internal ballistics were the MEOP, the mass flux, the port-to-throat ratio and the L/D (Length-to-Diameter) ratio.

When hot gases at high velocity or with a very high mass flow from the upper grains pass over the surface of the lower grains, there is a local increase in the burn rate of the propellant. This phenomenon is called erosive burning, which shall be controlled or ideally avoided [4].

According to data obtained in [5], for engines with an internal pressure of 400–600 psi, the maximum recommended mass flux is 2 lb/s in for 400 psi and 2.5 lb/s in for 600 psi [5] through the propellant core.

The L/D ratio is the ratio between the length and the inner diameter of the combustion chamber. The higher the L/D value, the greater the erosive burning effect [4]. A value of approximately 12 is used as a threshold for this parameter. The L/D ratio for this engine is around 10.039 (1014/101), which is an acceptable value.

It is known that the port/throat ratio is the ratio between the areas of the grain core and the nozzle throat; the recommended ratio for this ratio, according to [4], is between 2 and 4 to avoid erosive burning by high gas velocity.

By observing the data obtained from the internal ballistics' simulations for this motor, it can be seen that the limitations of the motor were respected.

Parameter	OpenMotor
Port/Troat	3.70
Mass flux (kg/(m^2*s))	1199.09
Max. P0 (MPa)	5.47
Avg. P0 (MPa)	4.99
Max. thrust (N)	3847.27
Avg. thrust (N)	3452.00
Total impulse (N-s)	10773.34
Specific impulse (s)	121.29
Burnout time (s)	3.09

Thrust time (s)	-
-----------------	---

Table 1: Results obtained from the internal ballistic simulations.

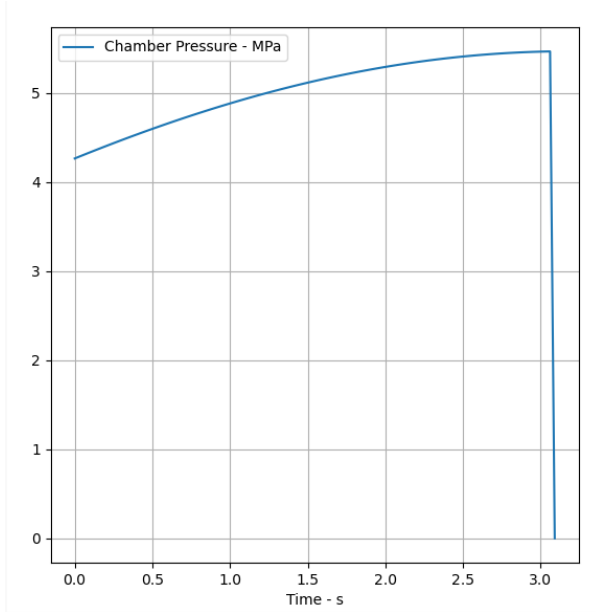


Fig. 31: Pressure-time graphic from OpenMotor

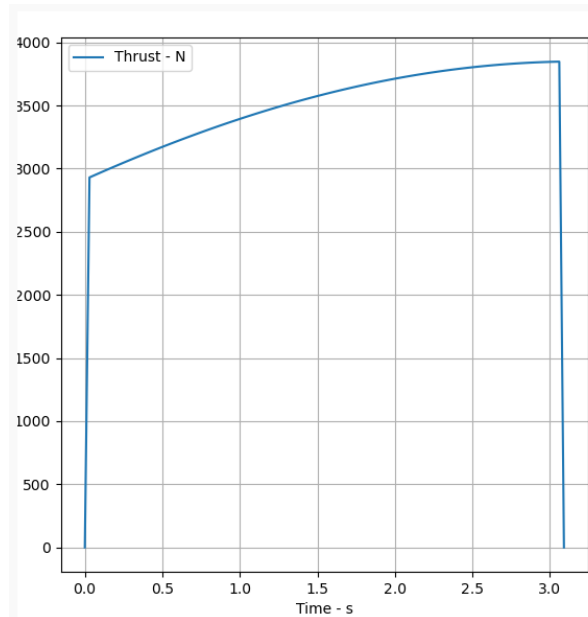


Fig. 32: Thrust-time graphic from OpenMotor.

Propellant

The propellant used in this rocket motor is KNSB, composed of a mixture of 65 % potassium nitrate and 35 % sorbitol by mass. The manufacturing can be found in the Appendix. process consists of heating both components and forming a colloid. The mixture is then molded into a tubular shape. More information about this process



Fig. 33: Propellant Grain [7]

Igniter grain

The igniter is used to ignite the propellant, this component consists of approximately 4 g of charge formulation [6] and a finger glove. The set is wrapped with masking tape, and the ends are sealed with insulation tape after inserting the e-match into the squib and is integrated to the line of fire. This component is used in redundancy, that is, two igniter grains are used, and they are arranged in parallel.

D. Avionics

The avionics system for Team Indra's subscale rocket, named *Vidyut* — derived from the Sanskrit word for electricity—features two independent setups: a COTS system and an SRAD system, ensuring redundancy. The SRAD system comprises two microcontrollers, a 6-DoF IMU, a barometric pressure sensor, a GPS module, a telemetry module, and a flight camera. Sensor data is processed through filtering and passed to an FSM that controls recovery events. Additionally, the data is logged onto an SD card and transmitted to the ground station in real-time. The primary functionalities of both systems are outlined below.

1. COTS System

The COTS system acts as the primary set of electronics to ensure the safe recovery of the rocket. EasyMini has been chosen as the primary altimeter, and the Featherweight GPS tracker as the primary GPS module.

Sl. No.	Name	Role	Basic information
1.	EasyMini	Altimeter	<ul style="list-style-type: none"> • Max altitude - 100,000ft³ • Main and drogue deployment • Small form factor • Easy post-flight data analysis using AltosUI
2.	Featherweight GPS tracker	GPS tracker	<ul style="list-style-type: none"> • Max altitude - 262,000ft⁴ • No directional antenna is needed • Can run for 16 hours on a small, 400mAh single lipo cell ^[2]

COTS BATTERY SPECIFICATIONS

The manufacturers of the COTS components have specified proprietary batteries to ensure optimal performance and integrity of the components. Efforts were made to ensure that the battery requirements stated by the manufacturers are in line with the rules laid down in the DTEG. The requirements are mentioned below:

Features	EasyMini	Featherweight GPS
Types/configuration	LiPo (recommended by the manufacturer) ⁵	LiPo (recommended by the manufacturer) ⁶
Nominal voltage	3.7V	3.7V
Battery capacity	400mAh	400mAh
Tested battery life	-	4-6 hours

³ <https://www.apogeerockets.com/Electronics-Payloads/Dual-Deployment/EasyMini>

⁴ <https://www.featherweightaltimeters.com/featherweight-gps-tracker.html>

⁵ https://altusmetrum.org/AltOS/doc/easymini.html#_in_the_rocket

⁶ <https://www.apogeerockets.com/Electronics-Payloads/Electronics-Accessories/400mAh-LiPo-Battery>

2. SRAD System

The SRAD (Smart Recovery and Data Logging) system is designed to perform four key functions essential for the successful operation of the flight computer. This system utilizes a 4-layer PCB constructed exclusively with Surface Mount Technology (SMT) components and implements two microcontrollers to enhance performance and reliability. The primary functions of the SRAD system are as follows:

1. **Real-time Apogee Detection** - This function is achieved by applying appropriate filters to the sensor data, effectively minimizing noise and employing mathematical models for accurate detection of apogee.
2. **Precision Recovery System Activation** - The system ensures reliable and precise triggering of the recovery mechanism, facilitating a successful and smooth recovery process.
3. **Comprehensive Data Logging and Telemetry** - Through robust data logging and telemetry capabilities, the SRAD system enables comprehensive analysis of flight performance, providing valuable insights for future improvements.
4. **Active Control System** - During the coasting phase, the deployment of an active airbrake system optimizes flight dynamics, enhancing overall control and stability.

Key Requirements

The SRAD system is designed with simplicity, responsiveness, and accuracy in mind. It incorporates checks and redundancies in both hardware and software to ensure reliable operation throughout the flight.

Additionally, I have implemented a code for apogee prediction, further enhancing the system's capability to anticipate critical flight events.

SRAD Electronic components:

1) Microcontrollers:

- **ESP32-S3-WROOM-1U-N16R8:** The dual-core microcontroller based on the Xtensa 32-bit LX7 microprocessor provides significant advantages for flight computer applications, especially in sensor data acquisition. Its dual-core architecture and clock speed of up to 240 MHz enables rapid processing and real-time decision-making, crucial for dynamic flight conditions. With 16MB flash and 8MB PSRAM, it efficiently manages firmware and extensive data logging without performance bottlenecks. This microcontroller ensures reliable real-time processing while maintaining power efficiency.

- **ESP32-S3-MINI-1U:** The dual-core microcontroller, based on the Xtensa 32-bit LX7 microprocessor with clock speeds up to 240MHz, is well-suited for a rocket's control system. Its dual-core architecture allows the efficient execution of complex control algorithms for precise adjustments. With 8MB of flash memory, it reliably stores control system firmware and operational parameters.

2) Sensors:

- **LPS22HHTR:** The LPS22HHTR is a compact, piezoresistive absolute pressure sensor functioning as a digital barometer, covering our full operational range. Utilizing I2C for communication and employing its internal filter, the sensor provides a 24-bit pressure data output with an ODR of up to 200 Hz and can withstand shocks up to 22,000 g.
- **IIM-42653:** The IIM-42653 is a 6 DoF MEMS IMU featuring a 3-axis accelerometer and 3-axis gyroscope. Utilizing SPI for high-speed data transfer, it offers an output data rate of up to 32 kHz. The accelerometer's programmable full-scale range extends up to $\pm 32\text{g}$, well beyond the expected acceleration forces experienced by our rocket.

3) Telemetry module:

- **RYLR993:** The telemetry module, working on LoRa technology, provides reliable wireless communication in the 868MHz and 915MHz frequency bands. Boasting an RF sensitivity of -148dBm, it's capable of achieving a range up to 16 km in outdoor line-of-sight conditions. Utilizing the UART communication protocol, this range significantly exceeds the requirements for our rocket's maximum altitude of 10,000 ft, ensuring a robust and reliable connection.

4) GPS module:

- **Antenova M20050-1:** The GNSS receiver module supports GPS, GLONASS, Galileo, and Beidou, featuring a MediaTek MT3333 flash chip and an internal antenna. It offers low current consumption, utilizes an Embedded Assist System for quick positioning, and communicates via UART. Furthermore, it provides up to 10 readings per second, enabling high-resolution location tracking for our application.

5) Camera module:

- **RunCam Split 3:** The RunCam Split 3 module records at 1080p at 60FPS and stores data into an Secure Digital card which is connected to its Digital Video Recorder board.

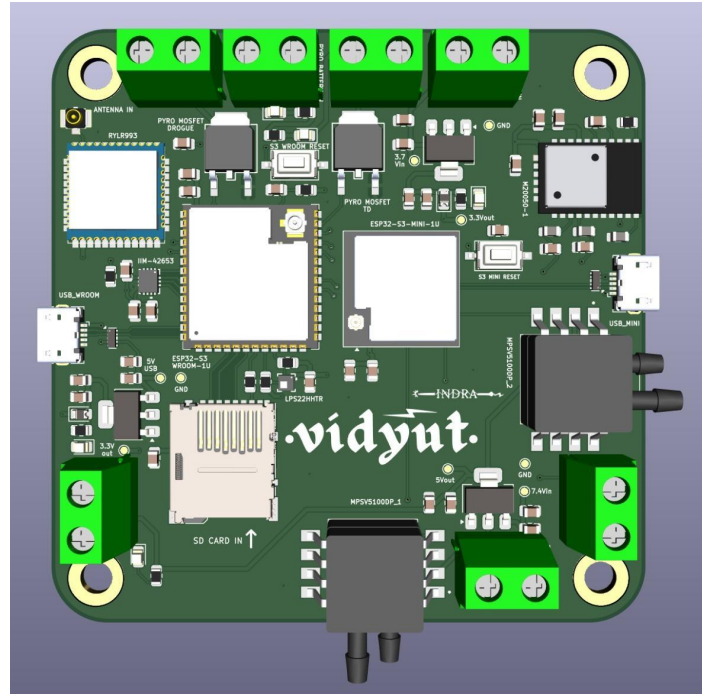


Fig 34: Flight Computer PCB

Software:

The SRAD system's software is designed to efficiently sample and filter sensor data, estimate states, and provide inputs to the FSM to trigger various events at designated points during flight. The software architecture is optimized to leverage the multiple cores of the ESP32-S3-WROOM-1U, with Core 0 dedicated to data acquisition and logging, while Core 1 handles filtering and necessary calculations. During flight, data will be temporarily stored in the PSRAM of the ESP32-S3-WROOM-1U and transferred to the SD card at every state transition.

The ESP32-S3-MINI-1U is reserved for interfacing with the pitot tube and managing control systems. The software also integrates airbrake functionality, allowing for precise control and stabilization during recovery operations based on the processed sensor inputs.

Additionally, the software supports real-time transmission of sensor data to the ground station for monitoring and analysis. For data filtering, the system employs the Madgwick filter⁷ for the IMU and a digital Butterworth filter for pressure data, enhancing the built-in filtering capabilities of both the IMU and pressure sensor.

FSM Structure

⁷ https://courses.cs.washington.edu/courses/cse474/17wi/labs/l4/madgwick_internal_report.pdf

State	Trigger	Functions
STANDBY	Power on	-
LAUNCH	Acceleration in X axis > 0	Data collection and computation
COASTING	Vertical acceleration < 0	Data collection and computation, air brakes control
APOGEE	Pressure ascending for 15 readings & pitch angle or yaw angle between 85° and 95°	Data collection and computation, drogue parachute deployment
MAIN	Rocket altitude <= 457 m	Data collection and computation, main parachute deployment
RECOVERY	Gyroscope data (all axes) = 0	GPS coordinates transmission

Control systems

The airbrakes utilize a bang-bang control strategy and receive inputs such as the current altitude (derived from pressure data of LPS22HHTR), the dynamic pressure data from the pitot tubes, the temperature and the current orientation of the rocket (given by the Madgwick filter).

This information is then processed through a pre-calculated equation that incorporates density as a function of altitude, which was developed using MATLAB using the ISA+15 model. The velocity is calculated using the isentropic formula for compressible flow⁸

$$V_1^2 = \frac{2a_1^2}{\gamma-1} \left[\left(\frac{p_0 - p_1}{p_1} + 1 \right)^{\frac{\gamma-1}{\gamma}} - 1 \right]$$

where,

V_1 = velocity

a_1 = speed of sound

γ = Heat capacity ratio

p_0 = total pressure

p_1 = dynamic pressure

The apogee is predicted using a hand-derived formula:

$$\text{apogee} = f^{-1}(g(\text{currentVelocity}) - g(0) + f(\text{currentAltitude}))$$

$$\text{where } f(s) = 3.4338 \cdot 10^{-9} \cdot \frac{s^3}{3} - 1.0595 \cdot 10^{-4} \cdot \frac{s^2}{2} + 1.1645 \cdot s$$

⁸ Introduction to flight by John D Anderson, pg 176

$$\text{and } g(v) = \frac{2m}{A \cdot Cd} \ln(v)$$

The complete derivation can be referred to in the appendix.

Ignition System

The ignition system comprises two primary components: the Ground Station and the Launchpad Station, both of which utilize the JB93 PCB.

At the Ground Station, there are two key safety switches: an ARM switch and a LAUNCH switch. The ARM switch is a keyed safety switch, ensuring that ignition cannot be initiated without authorized activation. The LAUNCH switch is a flip-type switch, which serves as the final command for ignition. The system follows a strict operational sequence, preventing unintended activation unless the ARM switch is engaged first.

For communication, the Ground Station is equipped with a 900 MHz antenna, enabling wireless data transmission between the Launchpad Station and the Ground Station. Additionally, telemetry and system data from the Testbed Station are relayed to a laptop via a USB connection from the JB93 PCB, allowing real-time monitoring and control.

At the Launchpad Station, there are two pre-arming flip switches that must be engaged before the final ARM and LAUNCH commands can be executed. These switches are wired to power MOSFETs, which are mounted on a prototyping board to facilitate easy replacement. The MOSFETs, load cell, and pressure transducers are powered by dedicated battery units, ensuring independent operation.

The JB93 PCB features two analog input channels, which are connected to a load cell and a pressure transducer for real-time data acquisition.

To enhance system reliability, both the Ground Station and Launchpad Station are equipped with SD card storage, providing redundancy for critical data logging.

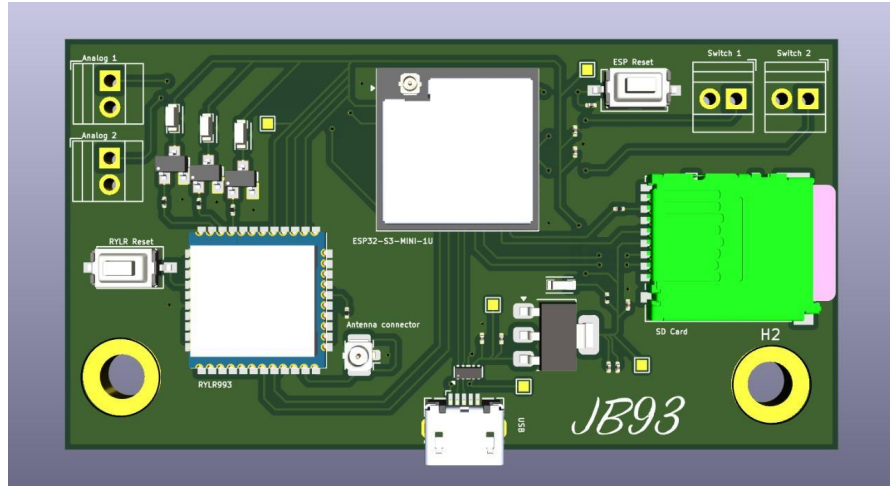


Fig. 35: Ignition System PCB (JB93)

SRAD Plotter

The SRAD plotter is made using python as it can handle and visualize live data more effectively than other languages. The SRAD plotter features 2 distinct operational modes –

1. Default mode – this mode enables real time plotting of live sensor data while simultaneously logging incoming data into a csv file for later analysis. This capability is particularly valuable for testing, demonstration purposes and post-flight data review.
2. CSV mode- this mode allows users to plot and visualize pre-recorded datasets from a csv file, offering a convenient method for analysing previously collected data.

In Normal Mode, the SRAD Plotter also records latitude and longitude data, which is stored within the data file. When the "Start GPS" function is activated, the application utilizes this stored GPS data to determine the rocket's precise location, facilitating efficient recovery operations.

With its robust data-handling capabilities and versatile operational modes, the SRAD Plotter serves as a highly reliable tool for real-time data monitoring, analysis, and mission-critical applications.

Avionics Setup

The design features a robust structure made from ABS plastic with a 20% infill, ensuring durability while maintaining a lightweight profile. It accommodates 11 batteries and various components, organized efficiently within two distinct walls: one dedicated to housing the components and antenna, and the other specifically designed for the batteries. Integrated slots

allow for seamless passage of wires to both the air brakes and recovery systems. With a diameter of 140 mm and a length of 220 mm, this assembly is compact yet functional.

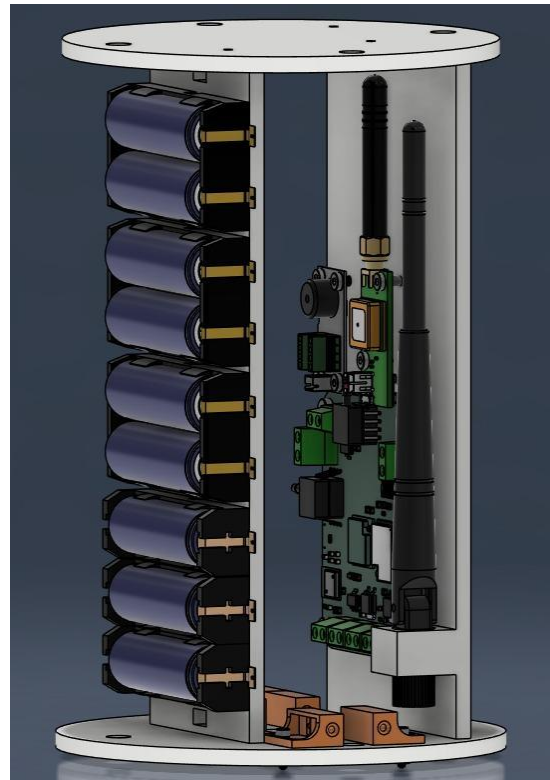


Fig. 36: Avionics Mount

E. Payload

AIRAWAT is a Non-Deployable Functional payload for Project Vajra. The payload is of CanSat form factor which resides in the nosecone of the rocket and the entire configuration weighs 3 kg (6.61 lbs) with length 35cm and Inner Diameter 12cm. The aim of the payload is to demonstrate and test a custom-built Stabilization System which uses a Gimbal Mechanisms to stabilize an aluminum platform which holds a Pyramid Object in its upside-down position on the bottom surface of the platform and the platform will be observed by a static camera mounted on the middle plate of the CanSat. The platform is rigidly attached to gimbal arms as well as with 3 helical extension springs placed 120° from each other and rigidly attached to the top plate of the CanSat. Since the platform being attached to the top plate through the helical springs will face vibrational forces coming from the CanSat and thus resulting in a wobbling motion (2 DOF namely Yaw and Pitch) about the center of platform and Roll will be restricted since the platform is rigidly attached to top plate of the CanSat through the Gimbal arm. The Payload idea is to minimize this wobbling motion and point the Apex of the object to the center of frame of the statically placed camera which records the entire process and stores its footage in a SD card.

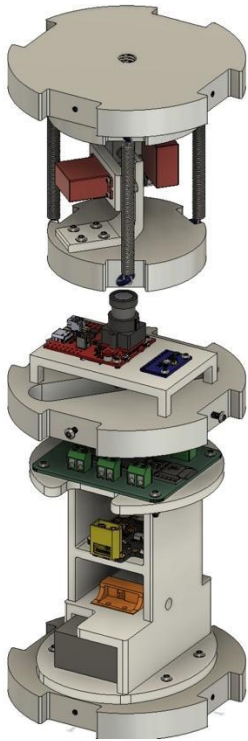


Fig. 37: Payload 3D Render

1. Components

- MPU9250 - Two MPU are used to get the orientation of the platform and the camera, and their output will directly feed into Teensy which will further be used to control the Gimbal Servos.
- Camera – The Camera used is OpenMV H7 plus which will be recording the entire process and storing it in a SD card mounted on the camera.
- Servos – For implementing Gimbal System, two 4 kgfcm (Torque Value) Positional (For better position control) Servos are used which will control 2 DOF of the Gimbal (Yam and Pitch).
- Micro-Controller – The entire operation will be carried on Teensy 4.1 i.e. reading MPU values, controlling the Gimbal System and triggering the camera to start recording as soon as launch is detected.
- Power Distribution Board – A PDB with built in BEC will be used to distribute regulated 5V to Teensy 4.1 and direct (7.4V from battery) supply to power the Servos.
- Battery – A 5600mah 7.4V Pro-range battery is used which will power the entire payload.

2. Payload Operation Stages

A. Powered Off

- System is powered off and no power supply from battery to rest of system.
- Pull Pin switch is not activated and isolates battery and all the components.
- Teensy 4.1, Camera and Gimbal System are in dormant state and no power is being supplied to them thus making system idle

B. Pre-Trigger (Powered On)

- Pull pin has been ejected manually and system gets powered on.
- Teensy 4.1 gets power from PDB at 5V and starts executing predefined C script, servos get power at 7.4V but gimbal system is not actively working, and camera is not yet triggered thus in dormant state.
- Both the MPU's (Platform and Camera) value are being monitored by Teensy for when to initiate the gimbal mechanism and camera.
- System in waiting state and once threshold value is crossed the trigger is activated.

C. Post-Trigger (Launch Detected)

- Once the threshold is crossed, indicating launch Teensy sends a signal to camera to start recording.
- After Triggering, Gimbal System Control part of the C++ script gets activated thus controlling the gimbal in real time according to the values incoming from both the MPUs.
- Gimbal from now on will be actively controlling the platform to make sure camera and pyramid apex are in LOS

3. Computation

The gimbal control system is implemented using the Teensy 4.1 onboard, which will manage the entire operation. The Teensy will be powered after pulling the PULL-PIN switch and will start to run a C++ script which will monitor orientation values coming from both the MPUs (MPU_Platform and MPU_Camera) after getting filtered through a complimentary filter designed to give more weightage to gyroscopic values and will trigger the camera to start recording and gimbal system to start working as soon as launch is detected. Detection of launch

will be confirmed by Accelerometer values coming from both the MPUs and will be crosschecked before Triggering camera and Gimbal System.

After launch is detected, the Teensy 4.1 will be actively controlling the Gimbal System to orient the platform in such a way that Object mounted on platform is in Line of Sight of camera. It will be doing this by taking MPU_Platform values and comparing them with those calculated by MPU_Camera, error calculated for both yaw and pitch will be fed into a PID controller with the last error and time differential from last measurement and PID controller will give out appropriate angle values for both the servos to be at and PWM signal will be generated to be to control the servos.

Control Systems

One PID controller function is used two separate times to control both yaw and pitch separately for better control over both the servos. The control loop follows standard PID formula.

$$Output = (K_p \times error) + (K_i \times \sum error) + (K_d \times d(error)/dt)$$

The yaw and pitch errors are computed as the difference between the platform's and camera's filtered angles from both the MPUs. P (Proportional) term scales the error thus providing the immediate correction, I (Integral) term accumulates the past errors (yawIntegral and pitchIntegral), counteracting steady-state errors and D (Derivative) term uses the difference between the current and previous errors (lastYawError and lastPitchError) to dampen oscillations.

The calculatePID() function computes the control output, which is then mapped to servo angles within the range of 0-180 degrees using the normalizeAngle() function. This ensures smooth and accurate adjustments to keep the camera aligned with the platform thus keeping the Apex of the pyramid object in LOS of the camera's centre.

After obtaining the error values and applying PID over them, they are constrained to 180° and desired angle for yaw and pitch is found out which will be used to turn the servos to the required position to keep platform steady.

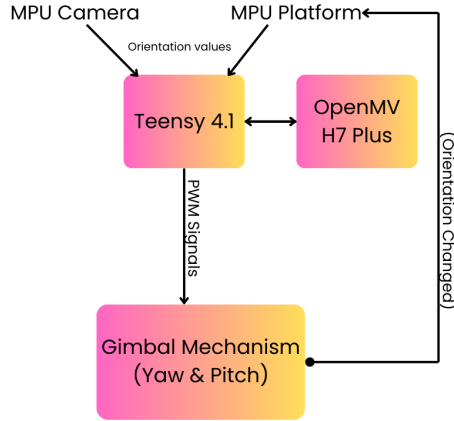


Fig. 38: Computation Logic (Workflow)

4. Electronics

The electronics system is built around a custom-designed PCB, DHRUVA, which houses the Teensy 4.1 microcontroller and features seven screw terminal blocks for secure connections under high G-forces during ascent. The PCB receives a 5V regulated supply from the BEC of the PDB, powered by a 5600mAh 7.4V 2S-2P Li-ion battery with 18650 cells. The PDB provides 5V regulated power to both the Teensy (through the PCB screw terminal) and the OpenMV camera (not structurally attached to the PCB), while the servos draw power from the direct 12V pad on the PDB, operating at 7.4V in this setup and their ground is connected to Teensy.

Both the MPU9250 (Camera and Platform) sensors are connected to the Teensy 4.1 via the PCB screw terminals for power ($V_{in}=3.3V$, GND) and I2C (SDA, SCL) communication, continuously sending data from the Pre-Trigger Stage to be used by the Teensy to control the Gimbal System. The camera is powered through the 5V line from the PDB's BEC, with its ground connected to the Teensy. Communication between the camera and Teensy uses UART (RX, TX) for triggering the camera in the Post-Trigger Stage, also connected via PCB screw terminals. PWM signals from the Teensy control the servos of the Gimbal System.

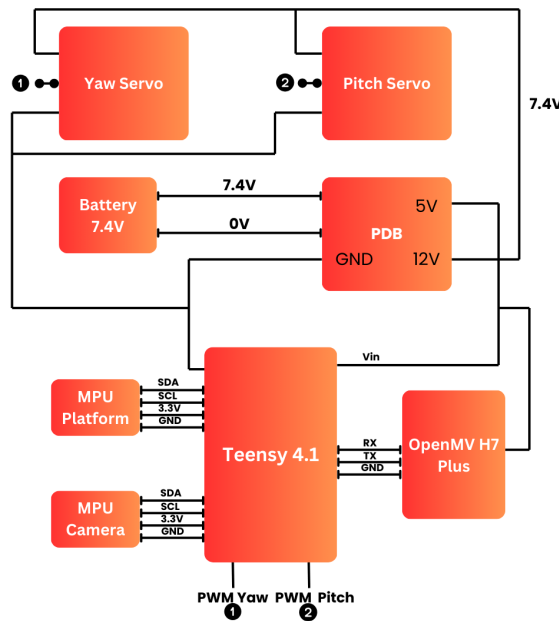


Fig: 39: Circuit Diagram

The payload's PCB is made of FR4 material with copper traces and is a 2-layer design. Trace widths are determined using a PCB trace width calculator based on current requirements, and all traces feature obtuse angles to enhance signal integrity and reduce static charge buildup. The PCB has an SMD LED to indicate power to the Teensy, with a resistor in series. The circuit uses a pull-pin switch to manually power the payload, keeping it in a dormant state to save battery until activated.

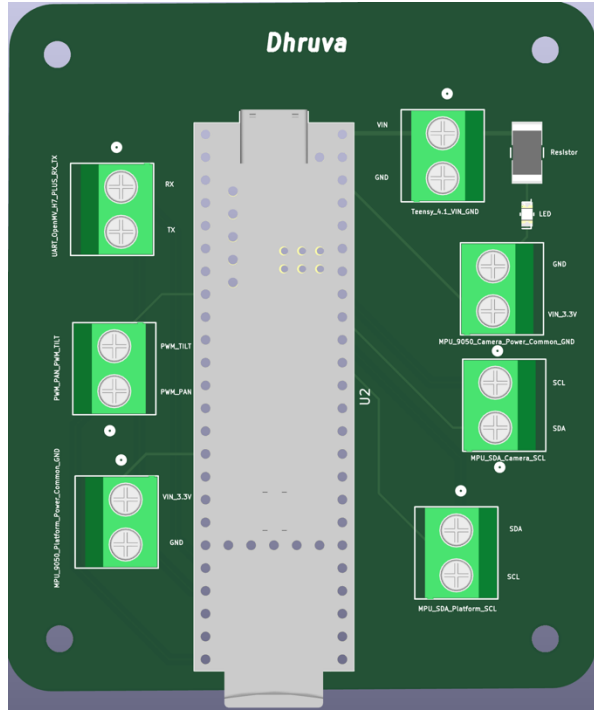


Fig. 40: Dhruva PCB 3D Render

5. Payload Camera

To capture the entire process and use the camera's frame center as a reference for positioning (with an offset for the camera's frame relative to the MPU), the OpenMV H7 Plus camera (resolution: 640x480, frame rate: 60fps, built-in microcontroller: STM32H743, 16MB of Flash storage, supports Micro Python) has been chosen. This camera is selected for its ability to remain idle until explicitly triggered to record. It features a built-in microcontroller acting as an interface between the Teensy and the camera sensor. When powered, the camera stays dormant until triggered by a signal from the Teensy via a UART connection. Upon triggering, it runs pre-built Micro Python code to begin recording and stores footage on a microSD card. This footage can later be used to analyze the payload's performance. Additionally, the OpenMV H7 Plus camera has a built-in visible light LED that can be used for basic illumination in low-light conditions, though it is not infrared.



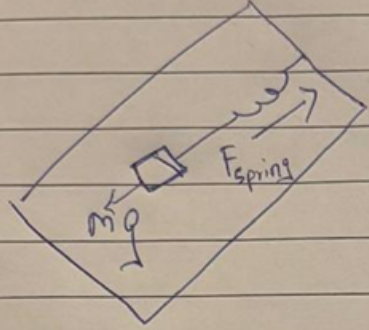
Fig 41: OpenMV H7 plus Camera

6. Mechanics of Spring Suspended Gimbal System

Main Platform and Springs

The Main Platform serves as the foundation which holds the pyramid object upside down on the bottom surface. Three springs are placed 120° apart, structurally attaching the platform to the Top Plate of the CanSat. The springs transfer vibrations generated during the rocket's ascent, allowing the platform to move in two rotational axes.

The decision to use three identical springs was made based on analysis with both four and two springs. When four springs were used, the platform would mainly exhibit linear motion rather than significant rotational motion, which was not desirable. The aim was to allow the platform to have considerable rotational motion in at least two axes. On the other hand, when only two springs were used, we believe the platform will fail to stabilize even under minimal vibrations, resulting in unstable motion. Additionally, the motion in this configuration proved difficult to dampen effectively with the gimbal system implemented in the payload. Thus, three springs provided an optimal balance, enabling the platform to maintain desired rotational movement while ensuring stability. The three springs are arranged 120° apart, which is the most optimal configuration for ensuring platform stability in the absence of external forces. This symmetrical placement distributes tension evenly, preventing unwanted tilting or displacement while allowing controlled rotational motion when forces are applied.



$$F_{\text{spring}} = K_{\frac{T}{T}} \cdot x$$

where $K_{\frac{T}{T}}$ = Spring constant
 x = spring extension

$$\text{So then: } -K_{\frac{T}{T}}x + mg + m(11g) = 0$$

$$\text{So: } K_{\frac{T}{T}}x = m(g + 11g)$$

→ if considering we want a maximum extension of the springs to be around 30mm and the load carried by the springs to be around 180grams

$$\text{then } x \approx 30 \text{ mm}$$

$$m = 180 \times 10^{-3} \text{ kg}$$

$$g = 9.80665 \text{ ms}^{-2}$$

$$\text{so: } K_{\frac{T}{T}} = \frac{180 \times 10^{-3} (12 \times 9.80665)}{30}$$

$$= 0.7060788$$

→ Since 3 springs are to be used,
 then $K_{\frac{T}{T}} = K_1 + K_2 + K_3 = 0.7060788 = 3K$

$$K \approx 0.2353596 \text{ N/mm}$$

Fig. 42 Spring Calculations

Looking at the Figure above on the calculations done, it was concluded that with the arrangement of the 3 springs, we believe that the optimal maximum extension of the spring should be around 30mm and hence we figured out the optimal spring constant of each spring should be around 0.235 N/mm. Due to the lack of proper research time, mwcomponents was selected as the manufacturer of these standard springs due to their vast library of standard springs and ease and quickness of delivery. From there we figured that 80662SCS Stainless Steel Extension spring was the most optimal for our case with its spring constant being 0.23 N/mm with a length of 50.8 mm and maximum predicted length of spring to be around 78.7 mm. Due to all these parameters mentioned, this spring would suit best for our payload as its spring constant is well close to our desired spring constant and its length is shorter than the length of the entire gimbal system which is around 66mm and hence the springs would be loaded even when static to provide with maximum movement as possible.

The topside of the platform mounts a MPU9250 which will provide the orientation of the platform in real time thus giving the position of the pyramid object which will be used as input to Teensy for further control of gimbal system.

Gimbal System

The Gimbal System comprises of two lightweight mini servos arranged to independently control the platform's yaw and pitch. It is constructed using three L-brackets, with each servo mounted to a bracket using screws, while one bracket is dedicated to securing the platform. The servos operate independently, ensuring that one's movement does not influence the other, allowing for two distinct degrees of freedom. This separation enhances precise control of the platform. The gimbal is rigidly fixed to the top plate using four screws, ensuring structural stability during operation.

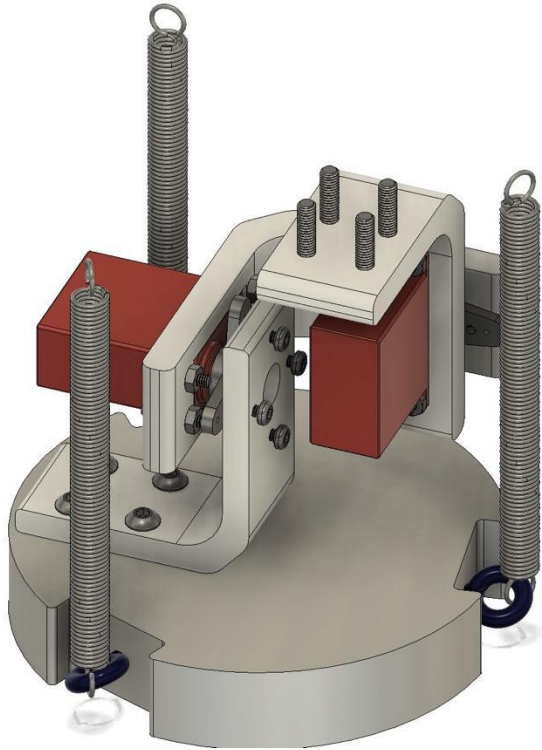


Fig 43: Platform with Gimbal System and Springs Mounted

F. Management

1. Inspiration for design

The team name, ‘INDRA’ , is inspired by one of the strongest and mightiest gods in Hindu mythology, the god of rain and thunder, Lord Indra. He is associated with the sky, lightning, weather, thunder, storms, rains, river flows, and war.

The rocket name, ‘VAJRA’ or the thunderbolt is the mighty weapon in the possession of Lord Indra.

Our payload is named Airavat, after the mount of Lord Indra.

Team Logo:

INDRA



Fig. 44

Rocket Name Logo:

VAJRA

Fig. 45

VAJRA Mission Patch:



Fig. 46

Payload Mission Patch:



Fig. 47

Team T-shirt:



Fig. 48

APPENDIX

1.1 Propulsion

Part	Item	Parameter	Value	Unit
Nozzle	Diameters	Throat diameter	26	mm
		Nozzle exit diameter	78	
	Lengths	Convergence length	49.271	mm
		Divergence length	245.044	
		Overall length	172.591	
	Angles	Nozzle convergence half angle	35	°
		Nozzle divergence half angle	12	
	Areas	Throat cross-section area	531	mm ²
		Nozzle exit cross-section area	4778.3	
	-	Nozzle expansion ratio	9.00	-
		Nozzle efficiency	0.85	%
Casing	Diameters	Casing ID	101	mm
	Lengths	Casing length	1086.5	
	Thickness	Casing thickness	6.5	
	Volumes	Casing volume (empty)	0.008704	m ³
Propellant	Mass	Total propelling mass	9.06	kg
	Diameters	Propellant outer diameter	95	mm
		Propellant core diameter	50	
	Lengths	Propellant segment length	240	mm
	Volumes	Propelling grain volume	0.004919	m ³
	Density	Grain density	1.749	g/cm ³
		Number of propellant segments	4	
		Maximum Kn	438.44	
		Combustion efficiency	93	%
-	Mass	Motor empty mass	12.32	kg
	Thrust	Average thrust	3452	N
	Impulse	Total impulse	10773.34	Ns
	-	Burn time	3.09	s
	-	Motor class	N	-

Charge Components	Percentage Composition
Manganese Dioxide (MnO ₂)	60
Aluminum (Al)	30
Sulphur	5
Guanidine Nitrate	5

Static Hot Fire Testing

In order to validate the rocket motor to comply with the Spaceport America Cup competition regulations, as outlined in section 5.17.5 of the IREC Design, Test, & Evaluation Guide document, a static hot-fire test must be conducted prior to the submission of the team's final design report. The thrust and pressure data are to be collected from the motor.

The N-class N3452 motor produces a total impulse of approximately 10773.34 Ns, has an outer diameter of 114 mm, a length of approximately 1199 mm, and a dry mass of 12.32 kg. Four grain propellant segments are used, totaling 9.06 kg. The propellant adopts the formulation outlined by the Ballistic Test and Evaluation System (BATES), with a 65/35 KNSB composition ratio by mass.

Each grain segment is 240 mm long, has an outer diameter of 95 mm and has a core diameter of 50 mm. Each of these grains is cast into a CFRP casting tube of length 240 mm, inner diameter 95 mm and thickness 1.5 mm.

Finally, there is the igniter, which initiates propellant burning. It consists of approximately 4 grams of ignition charge of the following composition: Manganese Dioxide (MnO₂) at 60% weight, Aluminum (Al) powder at 30% weight, Sulphur at 5% weight, and Guanidine Nitrate at 5% weight.

This formulation has a good burn rate and pressurizes the chamber effectively.

Propellant Casting Report

The standard formulation of KNSB propellant is 65% potassium nitrate (KN) which serves as the oxidizer and 35% Sorbitol (SB) which serves as the fuel and binder. This ratio of oxidizer to fuel mass represents a practical upper limit for "solids" loading of a sugar binder, while maintaining good performance and burn rate characteristics. A higher O/F ratio, and thus higher "solids" loading, may give slightly enhanced performance, but leads to a thicker consistency of the

melted mixture (slurry). This makes casting more difficult. The effect of using a lower O/F ratio is reduced performance and a slower burning rate. However, the slurry has a thinner consistency, which makes casting a bit easier.

Preparation

The first step in preparation of the propellant is to grind, or mill, the potassium nitrate to a fine texture. This may easily be done with the use of manual coffee grinder. Milling as such will reduce the particle size appreciably.

It should be noted that the viscosity of the melted propellant slurry is highly dependent upon how finely the potassium nitrate is milled.

For maximum performance, the sorbitol should be desiccated to remove all traces of residual water. This is done by placing sifted sorbitol in a shallow pan and putting in a desiccator for several days. It is important to note that desiccating should only be done if performance must be maximized. One drawback to desiccating the sorbitol is that it makes for a stiffer, more viscous propellant slurry when melted, making the casting operation more difficult.

Following the milling process, the two constituents are carefully weighed out using an accurate scale. Enough of the powdered mixture of potassium nitrate and sorbitol must be prepared to consider the inevitable waste resulting from the casting procedure, typically 20-25% additional for small batches, less for larger batches.

After individually weighing out the two constituents, the two are blended in a single container. Complete mixing of the two is necessary for optimum and consistent performance.

Casting:

- The casting process involves heating of the powdered mixture until it becomes molten, then casting into a mould to produce the propellant grain of the desired shape.
- The required temperature that the mixture must attain is just above the melting point of sorbitol.
- For KNSB, the casting temperature should be in the range of 115-125°C
- The casting procedure involves first preheating the deep fryer or skillet to the required temperature and maintaining this temperature +/- 5 degrees.
- Starting with about half the total amount, the powdered mix is added and stirred often to assist melting.
- Once this has melted, the remaining powdered mix is added.
- Stirring helps facilitate melting.

- The initial colour of the melted slurry is nearly colourless but begins to turn a white colour as the mixture becomes fully melted. Once all the powdered mixture has been fully incorporated into the melt, it is further heated and stirred, to eliminate any lumps that may be present.
- An additional five to ten minutes of heating will bring the slurry up to the casting temperature. If the sorbitol contains residual moisture (which is usually the case), melting occurs quite rapidly and the slurry has a pure white, almost translucent appearance. Some tiny bubbling may be noticed, as the residual water boils away. When nearly all the residual water has been driven off, the colour may begin to change to a light ivory. The purer the oxidizer, the purer white the colour of the slurry will be.
- In most cases the consistency will remain thick and must be simultaneously poured and scooped with a spoon or spatula onto the funnel.
- Pick up the mould then firmly tap it against a hard surface repeatedly. This serves to force any trapped air to rise to the surface.

Curing:

Sorbitol propellant remains pliable after cooling, and as such, a grain may become deformed if not carefully handled. A full day after casting, the exposed surfaces of the grain become quite hard. The inside, while still "waxy" and easily cut with a knife, is sufficiently rigid to allow handling. However, full curing may take a week. If it is demoulded too soon, the grain may become distorted when extracting the coring rod. Until fully cured, care should be exercised, as KNSB does tend to chip quite easily. After complete curing, however, the material becomes hard and relatively strong. It is perfectly acceptable to fire a grain any time after demoulding.

Surfactant as Casting Aid:

The use of a tiny amount of surfactant (a substance that tends to reduce the surface tension of a liquid in which it is dissolved) can greatly reduce the viscosity of molten KNSB. Molten KNSB becomes readily pourable when surfactant is incorporated, having a viscosity like maple syrup. Only a tiny amount of surfactant is required (~0.1% surfactant mass relative to the mass of the molten propellant).

Grain quality control

Bubbles in the grain can be a problem, since during the combustion of the propellant they make the surface exposed to irregular burning, as well as an increase in the burning area and, consequently, an increase in pressure is observed locally (in the region of the bubble). inside the combustion chamber.

Therefore, the engine works differently than expected and with results beyond expectations. To eliminate or alleviate this problem, the team performs a grain density control to find out if the grain produced would be suitable for use or not.

For quality controls, cracks can be analyzed using X-ray radiography, which is a non-destructive testing method that utilizes X-rays to identify cracks within a material by creating an image that reveals internal flaws, like cracks, voids, or inclusions, by exploiting the difference in how X-rays pass through areas of varying density within the material. The CAIF building at Manipal Academy of Higher Education (MAHE) offers access to its NDT lab for research.

2. Avionics:

Assumptions:

1. Cd of rocket remains constant in subsonic regions⁹
2. Angle of attack remains <2 degrees during ascent (from ORK data) and hence other components can be ignored

$$a = v \frac{dv}{ds}$$

$$F = ma = -\frac{1}{2}A \cdot Cd \cdot \rho \cdot v^2$$

$$-\frac{1}{2}A \cdot Cd \cdot \rho \cdot v^2 = mv \frac{dv}{ds}$$

Using curve fitting tool on MATLAB and using ISA+15 model,

$$\rho = 3.4338 \cdot 10^{-9} s^2 - 1.0595 \cdot 10^{-4} s + 1.1645$$

$$-\frac{1}{2}A \cdot Cd \cdot (3.4338 \cdot 10^{-9} s^2 - 1.0595 \cdot 10^{-4} s + 1.1645) ds = \frac{m}{v} dv$$

Integrating on both sides with upper limit as apogee and lower limit as current conditions,

$$-\frac{1}{2}A \cdot Cd \int_{\substack{\text{apogee} \\ \text{altitude}}}^0 (3.4338 \cdot 10^{-9} s^2 - 1.0595 \cdot 10^{-4} s + 1.1645) ds = m \int_{\substack{0 \\ \text{velocity}}}^{\infty} \frac{1}{v} dv$$

Rearranging,

$$\int_{\substack{\text{apogee} \\ \text{altitude}}}^0 (3.4338 \cdot 10^{-9} s^2 - 1.0595 \cdot 10^{-4} s + 1.1645) ds = \frac{2m}{A \cdot Cd} \int_0^{\infty} \frac{1}{v} dv$$

$$\left[3.4338 \cdot 10^{-9} \cdot \frac{s^3}{3} - 1.0595 \cdot 10^{-4} \cdot \frac{s^2}{2} + 1.1645 \cdot s \right]_{\substack{\text{apogee} \\ \text{altitude}}}^0 = \frac{2m}{A \cdot Cd} [\ln(v)]_0^{\infty}$$

⁹ Introduction to flight by John D Anderson, pg 294

$$\text{Let } f(s) = 3.4338 \cdot 10^{-9} \cdot \frac{s^3}{3} - 1.0595 \cdot 10^{-4} \cdot \frac{s^2}{2} + 1.1645 \cdot s$$

$$\text{Let } g(v) = \frac{2m}{A \cdot Cd} \ln(v)$$

$$f(\text{apogee}) = g(\text{velocity}) - g(0) + f(\text{altitude})$$

$$\text{Therefore, apogee} = f^{-1}(s)$$

$$f^{-1}(s) = \frac{\frac{y^2}{9x^2} - \frac{z}{3x}}{\sigma} - \frac{y}{3x} + \sigma \text{ [using MATLAB]}$$

$$\text{where } \sigma = \left(\sqrt{\left(\frac{s}{2x} - \frac{y^3}{27x^3} + \frac{yz}{6x^2} \right)^2 - \left(\frac{y^2}{9x^2} - \frac{z}{3x} \right)^3} - \frac{y^3}{27x^3} + \frac{s}{2x} + \frac{yz}{6x^2} \right)^{\frac{1}{3}}$$

$$\text{and } x = \frac{3.4338 \cdot 10^{-9}}{3}, y = \frac{-1.0595 \cdot 10^{-4}}{2}, z = 1.1645$$